Intracellular calcium regulation among subpopulations of rat dorsal root ganglion neurons

Shao-Gang Lu[1], Xiulin Zhang[1] and Michael S. Gold[1,2,3]

[1]*Department of Biomedical Sciences, Dental School,* [2]*Program in Neuroscience and* [3]*Department of Anatomy and Neurobiology, Medical School, University of Maryland, Baltimore, Baltimore, MD 21201, USA*

Primary afferent neurons are functionally heterogeneous. To determine whether this functional heterogeneity reflects, in part, heterogeneity in the regulation of the concentration of intracellular Ca^{2+} ($[Ca^{2+}]_i$), the magnitude and decay of evoked Ca^{2+} transients were assessed in subpopulations of dorsal root ganglion (DRG) neurons with voltage clamp and fura-2 ratiometric imaging. To determine whether differences in evoked Ca^{2+} transients among subpopulations of DRG neurons reflected differences in the contribution of Ca^{2+} regulatory mechanisms, pharmacological techniques were employed to assess the contribution of influx, efflux, release and uptake pathways. Subpopulations of DRG neurons were defined by cell body size, binding of the plant lectin IB_4 and responsiveness to the algogenic compound capsaicin (CAP). Ca^{2+} transients were evoked with 30 mM K^+ or voltage steps to 0 mV. There were marked differences between subpopulations of neurons with respect to both the magnitude and decay of the Ca^{2+} transient, with the largest and most slowly decaying Ca^{2+} transients in small-diameter, IB_4-positive, CAP-responsive neurons. The smallest and most rapidly decaying transients were in large-diameter, IB_4-negative and CAP-unresponsive DRG neurons. These differences were not due to a differential distribution of voltage-gated Ca^{2+} currents. However, these differences did appear to reflect a differential contribution of other influx, efflux, release and uptake mechanisms between subpopulations of neurons. These results suggest that electrical activity in subpopulations of DRG neurons will have a differential influence on Ca^{2+}-regulated phenomena such as spike adaptation, transmitter release and gene transcription. Significantly more activity should be required in large-diameter non-nociceptive afferents than in small-diameter nociceptive afferents to have a comparable influence on these processes.

(Resubmitted 3 July 2006; accepted after revision 24 August 2006; first published online 31 August 2006)
Corresponding author M. S. Gold: Department of Biomedical Sciences, University of Maryland Dental School, 666 West Baltimore Street, Baltimore, MD 21201, USA. Email: mgold@umaryland.edu

Primary afferent neurons are heterogeneous (Priestley *et al.* 2002). This heterogeneity has been well documented in afferent structure (i.e. termination patterns on both central and peripheral targets), neurochemistry (i.e. transmitter and receptor systems) and neurophysiology (i.e. adaptation properties and axon conduction velocity). This heterogeneity reflects the fact that primary afferent neurons subserve a wide array of functions both afferent and efferent in an organ system that is also highly heterogeneous.

Calcium (Ca^{2+}) acts as a second messenger within neurons to regulate a diverse array of physiological processes including transmitter release, changes in excitability, enzyme activity and gene expression (Berridge *et al.* 2000). Consequently, the concentration of intracellular Ca^{2+} ($[Ca^{2+}]_i$) is tightly regulated and the mechanisms underlying its regulation are numerous (Berridge, 1998; Berridge *et al.* 2000; Thayer *et al.* 2002). Regulatory mechanisms include influx pathways (ion channels), efflux pathways (pumps and exchangers), mechanisms underlying uptake and release from intracellular stores (mitochondria and endoplasmic reticulum) and Ca^{2+}-binding proteins. Results from previous studies indicate that these regulatory mechanisms are differentially distributed among subpopulations of sensory neurons. For example, inhibition of Na^+/Ca^{2+} exchanger by replacing extracellular Na^+ with Li^+ results in an increase in resting $[Ca^{2+}]_i$ in most dorsal root ganglion (DRG) neurons, while a slowed decay of evoked Ca^{2+} transients is only observed in a subpopulation of DRG neurons (Verdru *et al.* 1997). In addition, while mitochondria have been shown to buffer 'large' Ca^{2+} loads in most DRG neurons (Werth & Thayer, 1994) they appear to influence the magnitude and decay of

 DOI: 10.1113/jphysiol.2006.116418

evoked Ca^{2+} transients in specific subpopulations of DRG neurons (Kostyuk *et al.* 1999). There also is evidence that 'calcium-induced calcium release' (CICR) contributes to evoked Ca^{2+} transients in a subpopulation of rat DRG neurons (Shmigol *et al.* 1995*b*). Importantly, however, there has been no systematic analysis of the regulation of $[Ca^{2+}]_i$ among subpopulations of sensory neurons. Therefore, the present study was conducted in order to determine (1) whether there are differences among subpopulations of sensory neurons with respect to both resting and evoked increases in $[Ca^{2+}]_i$; and (2) whether differences in the regulation of $[Ca^{2+}]_i$ among subpopulations of sensory neurons reflects a differential contribution of various $[Ca^{2+}]_i$-regulatory mechanisms.

Standard fura-2 ratiometric techniques were employed in order to monitor evoked changes in intracellular calcium level of acutely dissociated DRG neurons. Pharmacological techniques were employed in order to assess the relative contribution of various $[Ca^{2+}]_i$ regulatory mechanisms. Preliminary results from this study have been published elsewhere (Lu & Gold, 2005).

Methods

Adult (240–340 g) male Sprague-Dawley rats (Harlan, Indianapolis, IN, USA) were used for this study. Rats were housed in the University of Maryland Dental School animal facility in groups of three on a 12 : 12 light dark schedule. Food and water are available *ad libitum*. All the experiments were approved by the University of Maryland Dental School Institution Animal Care and Use Committee and performed in accordance with National Institutes of Health guidelines as well as guidelines established by the International Association of the Study of Pain for the use of laboratory animals in research. Rats were deeply anaesthetized for both tissue labelling and tissue harvest (details provided below). The depth of anaesthesia was assessed by monitoring for the presence or absence of corneal reflexes and withdrawal responses to noxious pinch of the handpaw. Respiration rate was also monitored. Supplemental anaesthesia was administered until animals were areflexive. Following tissue harvest, rats were killed by decapitation.

Chemicals and reagents

2-APB (2-aminoethoxydiphenylborate) and CPA (cyclopiazonic acid) were purchased from Calbiochem (La Jolla, CA, USA), DiI 1,1′-dioctadecyl-3,3,3′,3′-tetramethylindocarbo-cyanine perchlorate was purchased from Invitrogen (Carlsbad, CA, USA). Fura-2 acetoxymethyl (AM) ester and pluronic were purchased from TEF Laboratories (Austin, TX, USA). C28R2 conjugated to TAT to enable cell access was custom synthesized (GenScript Corp, Scotch Pains, NJ, USA). All other chemicals were purchased from Sigma-Aldrich (St Louis, MO, USA). Concentrations used were based on results from previous studies by other investigators. 2-APB (100 μM), CCCP (carbonyl cyanide *m*-chlorophenyl hydrazone, 10 μM), CPA (10 μM), ionomycin (10 μM), ryanodine (10 μM), fura-2 AM (2.5 μM) and pluronic (0.025%) were dissolved in DMSO (dimethyl sulfoxide) at concentrations at least 1000× final, stored at −20°C, and then diluted in bath solution immediately before use. C28R2 (2 μM), FITC-conjugated IB_4 (IB_4, 10 μg ml^{-1}), UTP (uridine 5′-triphosphate, 100 μM) were dissolved in distilled water at 1000× stocks. Capsaicin was dissolved in ethanol as a 1 mM stock. All other compounds were dissolved in bath solution directly.

Labelling of DRG neurons innervating the glabrous skin of the hindpaw

Prior to tissue harvest (>3 weeks), DRG neurons innervating the glabrous skin of the hindpaw were labelled with the retrograde tracer DiI. Labelling was performed as previously described (Gold & Traub, 2004). DiI was dissolved in DMSO (170 mg ml^{-1}) and diluted 1 : 10 in 0.9% of sterile saline. Diluted dye (10 μl) was injected subcutaneously under isoflurane anaesthesia with a 30 g injection needle; anaesthesia was induced with 6% isoflurane (Abbott Laboratories, North Chicago, IL, USA) and maintained with 1.5% isoflurane. DiI-labelled neurons were easily identified under epifluorescence illumination with a Texas-red filter set.

Cell dissociation

Rats were deeply anaesthetized with a subcutaneous injection of a mixture (1 ml kg^{-1} of 55 mg ml^{-1} ketamine, 5.5 mg ml^{-1} xylazine, and 1.1 mg ml^{-1} acepromazine) (ketamine was from Fort Dodge Animal Health, Fort Dodge, WI, USA; xylazine and acepromazine were from Phoenix Scientific Inc., St Joseph, MO, USA) and DRG neurons were prepared as previously described (Gold *et al.* 1996). Briefly, $L_{4\text{-}5}$ DRG ipsilateral to DiI injection were surgically removed, and desheathed in ice-cold culture media composed of 90% minimal-essential-medium (MEM; Gibco BRL, Gaithersburg, MD, USA), 10% heat-inactivated fetal bovine serum (FBS), 1× MEM vitamins and 1000 u ml^{-1} each of penicillin and streptomycin (MEM-COMP). DRG were incubated 45 min at 37°C in 5 ml MEM containing 0.125% collagenase P (Roche Bioscience, Palo Alto, CA, USA), 1× MEM vitamins and 1000 u ml^{-1} each of penicillin and streptomycin, and bubbled with carbogen (95% O_2–5% CO_2). DRG were centrifuged at ∼400 *g* for 4 min,

the collagenase solution was removed and then replaced 2.5 ml Ca^{2+}- and Mg^{2+}-free Hanks balanced salt solution (Gibco BRL, Gaithersburg, MD, USA) containing 0.25% trypsin (Worthington, Bristol, UK), 80 μg ml^{-1} DNase and 0.025% EDTA. Ganglia were mechanically dissociated in this solution with fire-polished pasteur pipettes and then incubated for 5 min at 37°C. Trypsin activity was inhibited by the addition of 2.5 ml MEM-COMP containing 0.125% $MgSO_4$. Cell suspension was then centrifuged at ~400 *g* for 4 min, resuspended with MEM-COMP, and plated onto glass coverslips, previously coated by a solution of 5 μg ml^{-1} mouse laminin (Gibco BRL, Gaithersburg, MD, USA) and 0.1 mg ml^{-1} poly-L-ornithine. The cells were incubated in MEM-COMP at 37°C, 3% CO_2, and 90% humidity for 2 h, at which point they were transferred to a L-15 media (Gibco BRL, Gaithersburg, MD, USA) containing 10% FBS, 5 mM Hepes and 5 mM glucose, and stored at room temperature. All experiments were performed within 8 h of tissue harvest.

Subclassification of DRG neurons

DRG neurons were subclassified on the basis of several criteria. These included cell body size, binding to the plant (*Griffonia simplicifolia*) lectin isolectin B_4 (IB_4) and responsiveness to the algogenic compound capsaicin (CAP). Neurons were divided into small (<30 μm), medium (30–40 μm), and large (≥40 μm) based on cell body diameter (Caffrey *et al.* 1992; Scroggs & Fox, 1992*a*) as measure with a calibrated eyepiece reticule. Based on the rough correlation between cell body size and axon conduction velocity (Harper & Lawson, 1985) as well as previous anatomical and electrophysiological studies performed *in vitro* (Lawson, 2002), neurons with a small cell body diameter are likely to be nociceptive afferents, while those with a large cell body diameter are likely to be non-nociceptive afferents. Neurons with a medium cell body diameter are likely to encompass both nociceptive and non-nociceptive afferents. IB_4 binding is a relatively simple way of identifying a unique population of afferents that appear to be involved in nociceptive processing (Nagy & Hunt, 1982; Silverman & Kruger, 1990). IB_4-positive (IB_4+) neurons tend to give rise to unmyelinated axons, be devoid of the neuropeptides substance P and calcitonin gene-related peptide (CGRP) and express a unique distribution of other receptors, including the ATP receptor $P_{2\times3}$ (Vulchanova *et al.* 1998), which is thought to mediate the pain associated with tissue damage. Finally, while not all nociceptive afferents are CAP responsive (CAP+), CAP+ neurons are likely to be nociceptive, given that the only sensation associated with the cutaneous application of CAP is pain, and in naïve tissue CAP only activates high-threshold C-fibre afferents (Martin *et al.* 1987).

Intracellular Ca^{2+} measurements

DRG neurons were loaded with 2.5 μM calcium indicator fura-2 AM ester with 0.025% pluronic for 20 min at room temperature as previously described (Thut *et al.* 2003). They were subsequently labelled with FITC-conjugated IB_4 (10 μg ml^{-1} for 10 min). Following fura-2 loading and IB_4 labelling, DRG neurons were placed in a recording chamber and were continuously perfused with normal bath solution (mM: 130 NaCl, 3 KCl, 2.5 $CaCl_2$, 0.6 $MgCl_2$, 10 Hepes, 10 glucose, pH adjusted with Tris base to 7.4, osmolality adjusted with sucrose to 325 mosmol l^{-1}). For some experiments, a 'Ca^{2+}-free' bath solution was employed, which was the normal bath solution modified by the omission of $CaCl_2$, the addition of 0.1 mM EGTA and an increase in the concentration of $MgCl_2$ 3.1 mM. Fluorescence data were acquired on a PC running Metafluor software (Molecular Devices, Sunnyvale, CA, USA) via a CCD camera (Roper Scientific, Trenton, NJ, USA, Model RTE/CCD 1300). The ratio (R) of fluorescence emission (510 nm) in response to 340/380 nm excitation (controlled by a lambda 10-2 filter changer (Sutter Instruments CA, USA)) was acquired at 1 Hz during drug applications. All drugs were applied via a gravity-fed chamber perfusion system except high K^+ (30 mM), caffeine (10 mM), and capsaicin (500 nM), which were delivered by a computer-controlled fast perfusion system (switching time <50 ms; ALA Scientific Instruments, Westbury, NY, USA, Model DAD-12); normal bath (with 2.5 mM Ca^{2+}) was applied with the fast perfusion system where indicated.

Intracellular free calcium concentration ($[Ca^{2+}]_i$) was derived from fluorescent ratios (R) following performance of *in situ* calibration experiments (Grynkiewicz *et al.* 1985; Kao, 1994) according to the following equation:

$$[Ca^{2+}]_i(\text{nM}) = K_d(S_{f2}/S_{b2})(R - R_{min})/(R_{max} - R)$$

where K_d is the dissociation constant of fura-2 for Ca^{2+} at room temperature (i.e. 224 nM); S_{f2}/S_{b2} is the fluorescence ratio of the emission intensity excited by 380 nm signal in the absence of Ca^{2+} to that during the presence of saturating Ca^{2+}; R_{min} or R_{max} is the minimal or maximal fluorescence ratios, respectively. R_{min} was measured by perfusing the neurons with nominally Ca^{2+}-free bath solution containing 1.0 mM EGTA and 10 μM ionomycin with 10 mM Mg^{2+} for at least 40 min. R_{max} was obtained by perfusing neurons with standard bath solution containing 20 mM Ca^{2+} and 10 μM ionomycin for a few minutes. Background values of F_{340} and F_{380} were collected by perfusing the neurons with 50 μM digitonin for a few minutes. Values of S_{f2}/S_{b2}, $R_{min,}$ or R_{max} were 15.51, 0.48, or 14.83 averaged over 65 neurons obtained from seven separate *in situ* calibration experiments performed over the time period during which all other experimental data was collected.

Electrophysiological recording

Whole-cell patch-clamp recordings were performed using an Axopatch 200B amplifier (Molecular Devices, Sunnyvale, CA, USA) or EPC-9 amplifier (HEKA Elektronik GmbH, Lambrecht, Germany). Series resistance was compensated (>80%) with amplifier circuitry. Data were acquired at 10 kHz and filtered at 2 kHz. Electrodes (1.8–3.0 MΩ) were filled with pipette solution (mM: 100 Cs-Methansulphonate (MS), 5 Na-MS, 40 TEA-Cl, 1 $CaCl_2$, 2 $MgCl_2$, 11 EGTA, 10 Hepes, 2 ATP-Mg, 1 GTP-Li); pH was adjusted to 7.2 with Tris-base and osmolality was adjusted to 310 mosmol l^{-1} with sucrose. The bath solution was constructed to minimize other currents in sensory neurons and contained (mM): 100 Choline-Cl, 30 TEA-Cl, 2.5 $CaCl_2$, 0.6 $MgCl_2$, 10 Hepes, 10 Glucose; pH was adjusted to 7.4 with Tris-base and osmolality was adjusted to 325 mosmol l^{-1} with sucrose. Neurons were held at −60 mV. Voltage-gated Ca^{2+} currents were evoked with a series of 60 ms command potentials from −80 to 60 mV in 5 mV increment steps following a 15 ms prepulse to −100 mV. Leak currents were digitally subtracted using a *P*/–4 leak subtraction protocol from a holding potential of −80 mV. For whole-cell current-clamp recording, electrodes were filled with the pipette solution mentioned above, but Cs^+ and TEA^+ were replaced by K^+, and neurons were perfused with normal bath solution.

Intracellular Ca^{2+} measurements from voltage-clamped DRG neurons

The perforated-patch configuration of whole-cell patch clamp was used to assess Ca^{2+} transients evoked with voltage steps. For these experiments, pipette solution contained (mM): 30 KCl, 55 K_2SO_4, 1 $MgCl_2$, 0.1 EGTA, 10 Hepes; pH was adjusted to 7.2 with KOH and osmolality was adjusted to 310 mosmol l^{-1} with sucrose. Electrodes (1.8–3.0 MΩ) were dip-filled in the pipette solution and subsequently back-filled with the same solution but containing Amphotericin B (480 μg ml^{-1}, Sigma-Aldrich, St Louis, MO, USA) for perforation (Usachev *et al.* 1995). A series resistance of <20 MΩ was achieved between 5 and 30 min after seal formation which was compensated (about 60%) with amplifier circuitry. Ca^{2+} transients were evoked with depolarization voltage steps from −60 mV to 0 mV for 4000 ms, the same duration used to apply high-K^+ solution.

Statistical analysis

Data are expressed as mean ± S.E.M. Student's *t* test and one-way ANOVA with the Holm–Sidak *post hoc* test were used for simple comparisons between groups. For experiments involving the application of test compounds, vehicle controls were always included. Because we sought to assess the presence of statistically significant influences of test compounds and the possibility that there were differences between subpopulations of sensory neurons with respect to the response to the test compound (i.e. two main effects), as well as the interaction between the two, a two-way ANOVA was employed. Differences between groups were assessed with a Holm–Sidak *post hoc* test if there was a statistically significant interaction between main effects. Statistical significance was assessed at $P < 0.05$.

Results

Subpopulations of DRG neurons studied

Acutely dissociated DRG neurons from adult male rats were classified based on the cell body diameter, IB_4 binding, CAP sensitivity and whether or not they innervated the glabrous skin of the hindpaw. Cell body diameter of DRG neurons was measured under bright-field illumination (Fig. 1*Aa* and *d*). DiI+ and IB_4+ DRG neurons were identified under epifluorescence illumination (Fig. 1*Ab* and *c*). CAP+ DRG neurons were identified at the end of experiments with a brief application of CAP (500 nM). Neurons considered CAP+ demonstrated an increase in fura-2 fluorescent ratio >20% above baseline (Fig. 1*Ae* and *f*). A histogram of cell body diameter is shown in Fig. 1*B*, and 55% (127 out of 231), 25% (57 out of 231) and 20% (47 out of 231) of all DRG neurons studied were classified as small, medium, and large. Consistent with previous observations (Harper & Lawson, 1985), this histogram was skewed, with the majority of neurons falling into the small-diameter category; the median cell body diameter was 28.8 μm (with 25.3 μm and 35.9 μm as 25th and 75th percentiles, respectively). 59% (136 out of 231) of neurons were IB_4+ and 53% (123 out of 231) of neurons were CAP+. The majority of both IB_4+ neurons (71%, 96 out of 136) and CAP+ neurons (69%, 85 out of 123) were classified as small, while 28% (39 out of 136) and 1% (1 out of 136) of IB_4+ neurons and 29% (36 out of 123) and 2% (2 out of 123) of CAP+ neurons were classified as medium and large, respectively. Thus, consistent with previous observations (Gold *et al.* 1996; Dirajlal *et al.* 2003), both IB_4+ and CAP+ neurons were significantly smaller than IB_4– and CAP– neurons. Seventy-one per cent (97 out of 136) of IB_4+ neurons were CAP+, while 79% (97 out of 123) of CAP+ neurons were IB_4+.

Twenty-three per cent (53 out 231) of the total population were DiI+ neurons (i.e. cutaneous neurons innervating glabrous skin of the hindpaw), which comprised 19, 16 and 18 small, medium and large neurons, respectively. The median cell body diameter of these cutaneous neurons was 31.23 μm (with 27.9 μm and 41.6 μm as 25th and 75th percentiles, respectively).

Fifty-one per cent (27 out of 53) of cutaneous neurons were IB_4+ and 49% (26 out of 53) were CAP+; 59% (16 out of 27) of IB_4+ cutaneous neurons and 58% (15 out of 26) CAP+ cutaneous neurons were classified as small. Thirty-seven per cent (10 out of 27) and 4% (1 out of 27) of IB_4+ cutaneous neurons, and 38% (10 out of 26) and 4% (1 out of 26) of CAP+ cutaneous neurons were classified as medium and large, respectively; 78% (21 out of 27) of IB_4+ cutaneous neurons were CAP+; 81% (21 out of 26) of CAP+ cutaneous neurons were IB_4+. There were no statistically significant differences between cutaneous neurons and unlabelled neurons with respect to the distribution of neurons within subpopulations.

High-K^+-induced Ca^{2+} transient in DRG neurons

A brief (4 s) application of 30 mM K^+ (high K^+) was used to evoke an increase in $[Ca^{2+}]_i$ subsequently referred to as a Ca^{2+} transient. Representative recordings in Fig. 2*A–C* show evoked Ca^{2+} transients in small-, medium- and large-diameter DRG neurons, respectively. These evoked Ca^{2+} transients were entirely dependent upon the presence of extracellular Ca^{2+} (Fig. 2*D*), as the 30 mM K^+-evoked Ca^{2+} transients were completely abolished in Ca^{2+}-free bath solution in all small (7 of 7), medium (3 of 3) and large (3 of 3) neurons tested. In order to determine the extent of the depolarization induced by high K^+, as well as whether differences in resting membrane potential and/or adaptation properties could contribute to differences between subpopulations with respect to the magnitude and decay of evoked Ca^{2+} transients, conventional whole-cell patch recordings were made in current clamp (Fig. 2*E*). Resting membrane potential was -56.4 ± 4.3 ($n = 10$), -58.5 ± 4.2 ($n = 10$) and -59.7 ± 3.1 ($n = 7$) in small-, medium- and large-diameter DRG neurons, respectively. Differences between groups were not statistically significant ($P > 0.05$, one way ANOVA). A 4 s application of 30 mM K^+ resulted in a rapid depolarization to a membrane potential at which the majority of neurons were rapidly 'clamped' for the duration of the high-K^+ application (Fig. 2*E*). Following termination of the high K^+, resting membrane potential was rapidly re-established. Action potentials were evoked by high-K^+ application in 15 of 27 (56%) neurons tested, which included 8 of 10 small-diameter neurons, 7 of 10 medium-diameter neurons and 0 of 7 large-diameter neurons. Only one action potential was fired in 6 of the 15 neurons in which any activity was observed. In four small-diameter neurons and one medium-diameter neuron in which more than one action potential was fired, overshooting action potentials were followed by high-frequency (44 ± 5 Hz) membrane potential oscillations that decreased in amplitude to undetectable levels over the initial period of membrane depolarization. The average time between the start of high-K^+ application and the point at which the membrane potential was effectively 'clamped' at a depolarized potential was 773 ± 193 ms in all the neurons that fired more than a single spike yet demonstrated accommodation during the high-K^+ application. This duration was 814 ± 173 ($n = 6$) and 528 ms ($n = 1$) in small- and medium-diameter neurons, respectively. Finally, in two neurons, the high-K^+-evoked

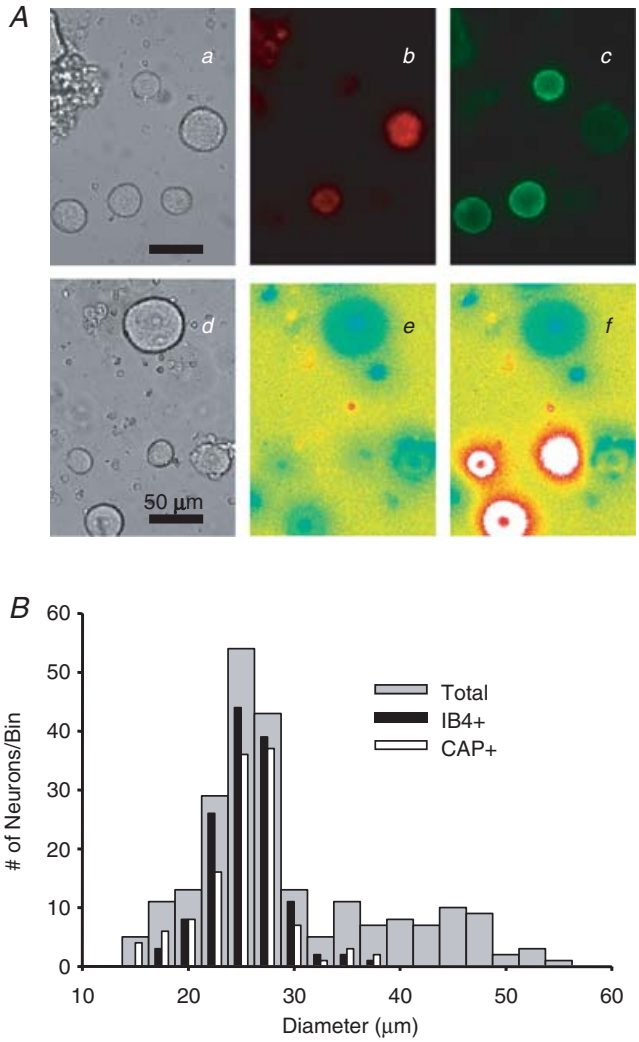

Figure 1. Subpopulations of DRG neurons
A, photomicrographs of subpopulations of DRG neurons. Bright field images (*a* and *d*) were used to determine cell body diameter (scale bars: 50 μm). Under epifluorescence illumination, DiI- (*b*) and IB_4- (*c*) labelled neurons were identified in the field of neurons shown in *a*. The capsaicin sensitivity of the neurons shown in *d* was assessed with fura-2 microfluorimetry. Fura-2 fluorescence ratio is low at rest (*e*) and dramatically increased in a subpopulation of neurons (*f*) following application of capsaicin (500 nM). *B*, cell body diameter histogram of the total population of DRG neurons ($n = 231$, grey bars), IB_4-positive (IB4+) neurons ($n = 136$, black bars) and CAP-sensitive (CAP +) neurons ($n = 123$, white bars). Appoximately 70% IB_4+ and CAP+ DRG neurons had a small cell body diameter.

depolarization was associated with sustained action potential generation; the average instantaneous spike frequency was ∼7 Hz in one and ∼4 Hz in the other. Both of these neurons were classified as medium-diameter neurons. Of the 25 neurons tested that did not fire sustained action potentials in response to 30 mM K^+, the membrane potential was effectively 'clamped' to -17 ± 1 mV, -19 ± 1 mV and -20 ± 1 mV in small, medium and large neuron groups, respectively. Differences between groups were not statistically significant ($P > 0.05$, one-way ANOVA).

Differences among subpopulations of DRG neurons with respect to evoked Ca^{2+} transient

The resting $[Ca^{2+}]_i$ levels were 145 ± 4 ($n = 127$), 129 ± 5 ($n = 57$) and 128 ± 4 nM ($n = 47$) in small-, medium- or large-diameter DRG neurons, respectively. They were 138 ± 3 ($n = 136$) and 137 ± 4 nM ($n = 95$) in IB_4+ and IB_4- neurons, respectively, and they were 135 ± 3 ($n = 123$) and 140 ± 4 nM ($n = 118$) in CAP+ and CAP– DRG neurons, respectively. Differences between subpopulations were not statistically significant ($P > 0.05$, one-way ANOVA or Student's t test).

As shown in Fig. 3*A*, the magnitude of evoked Ca^{2+} transient, analysed as the difference between peak evoked Ca^{2+} and baseline ($\Delta[Ca^{2+}]_i$), was largest in small- and smallest in large-diameter DRG neurons, respectively ($n = 127$, 57, and 47 for small-, medium-, and large-diameter neurons, respectively). Differences between groups were statistically significant ($P < 0.01$, one-way ANOVA). The decay of evoked Ca^{2+} transient (Fig. 3*A*), analysed as time to 50% of peak (T_{50}), was slowest in small- and the fastest in large-diameter DRG

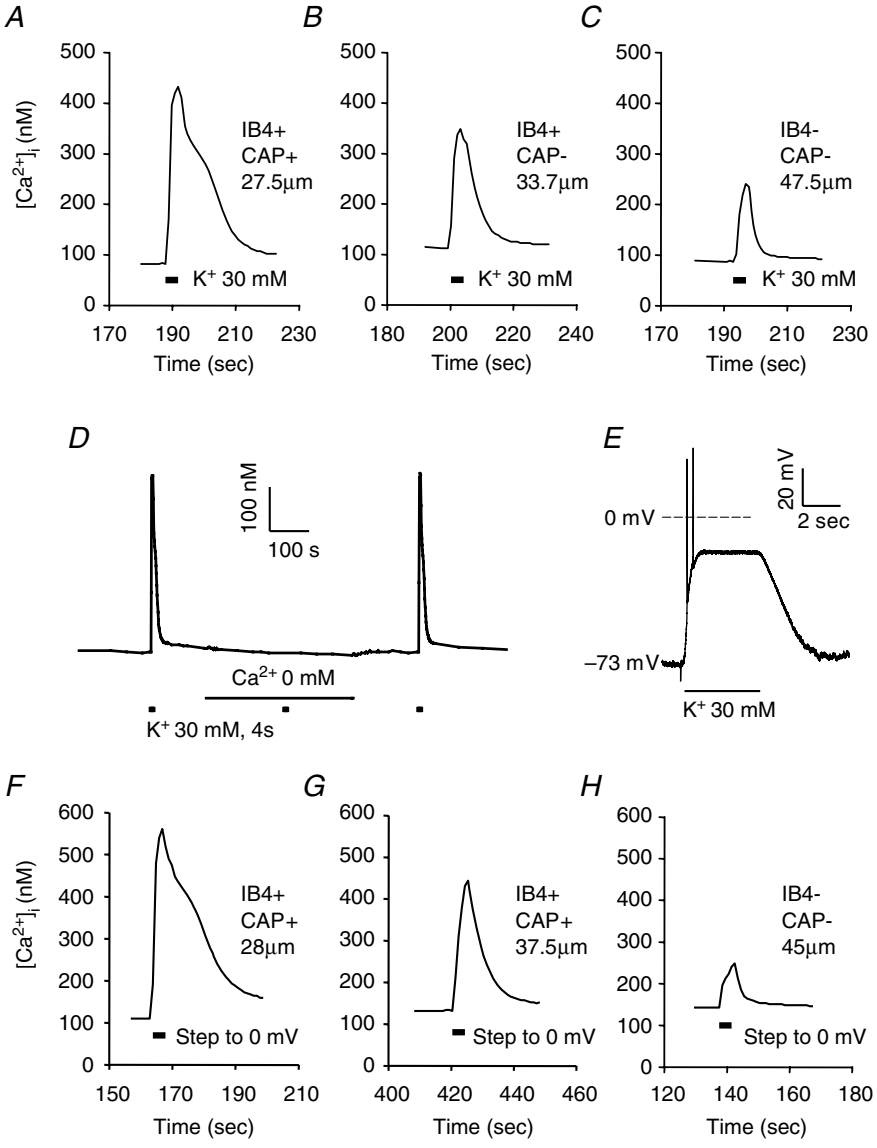

Figure 2. High-K^+-evoked Ca^{2+} transients in DRG neurons
Ca^{2+} transients were evoked with a 4 s application of 30 mM K^+ in typical small- (*A*), medium- (*B*) and large- (*C*) diameter DRG neurons. *D*, the high-K^+-evoked Ca^{2+} transient is abolished in the presence of Ca^{2+}-free bath solution. High K^+ was applied at points indicated by black bars. Ca^{2+}-free bath solution was applied for the time indicated with the continuous line. *E*, Response of a typical neuron under current clamp to 30 mM K^+ (high K^+). Voltage trace shows a rapid depolarization that was associated with the generation of two action potentials. The membrane potential was then stably 'clamped' at −21 mV for the remainder of the high-K^+ application, after which membrane potential returned to baseline. Perforated-patch recording was used to study the magnitude and decay of Ca^{2+} transients evoked with a voltage step. Ca^{2+} transients evoked with a 4 s voltage step to 0 mV from a holding potential of −60 mV in typical small- (*F*), medium- (*G*) and large- (*H*) diameter neurons were similar to those evoked with 30 mM K^+.

neurons. Differences between groups were statistically significant ($P < 0.01$, one-way ANOVA). The magnitude was larger and the decay was longer in IB_4+ ($n = 136$) than in IB_4- ($n = 95$) DRG neurons, respectively (Fig. 3*B*), while magnitude and decay were larger and longer in CAP+ ($n = 123$) than in CAP– ($n = 118$) DRG neurons, respectively (Fig. 3*C*). Differences between groups were statistically significant ($P < 0.01$, Student's t test). The evoked increase in $[Ca^{2+}]_i$ in subpopulations of cutaneous DRG neurons (DiI+) was qualitatively and quantitatively similar to that observed in subpopulations of unlabelled DRG neurons as shown in Fig. 3*D–F*. Differences between subpopulations of cutaneous neurons were statistically significant ($P < 0.05$ or $P < 0.01$, one-way ANOVA or Student's t test). However, there were no statistically significant differences between subpopulations of unlabelled and DiI-labelled DRG neurons with respect to the Ca^{2+} transients ($P > 0.05$, two-way analysis of variance). Because there were no differences between cutaneous and total DRG neurons with respect to the

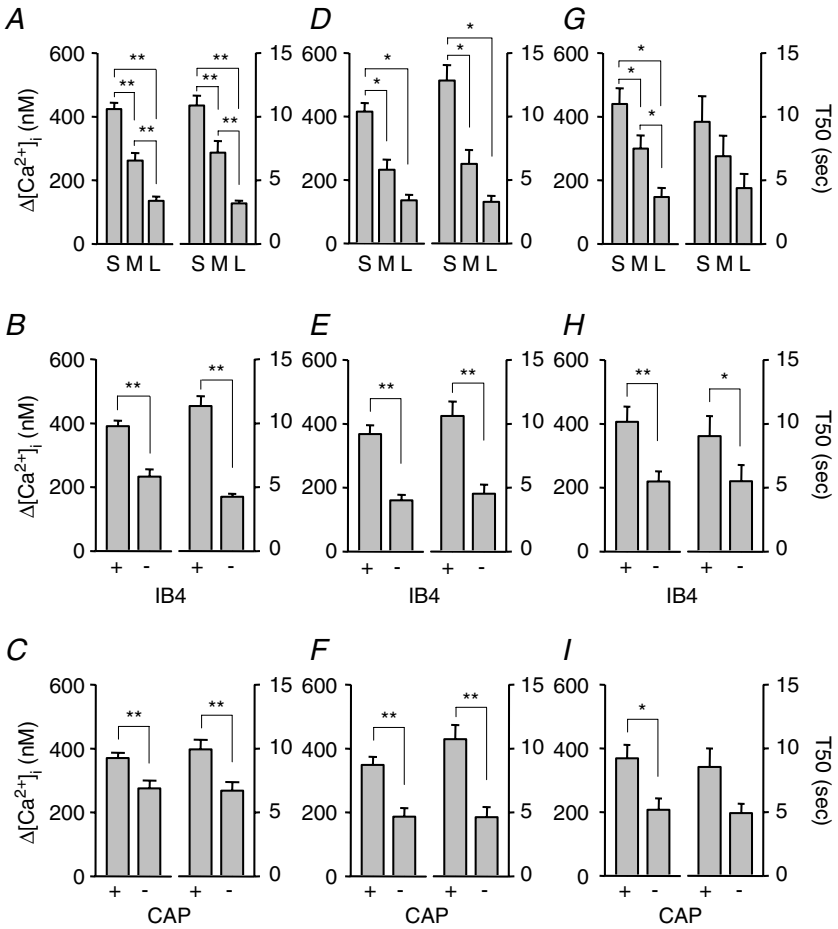

Figure 3. Differential distributions of evoked Ca^{2+} transients among subpopulations of DRG neurons
A, the magnitude (left), analysed as $\Delta[Ca^{2+}]_i$ (peak value – baseline), and the decay (right), analysed as time to 50% of peak (T_{50}), of evoked Ca^{2+} transients were the largest in small-, and the smallest in large-diameter neurons ($n = 127$ in small-, 57 in medium-, and 47 in large-diameter cell groups). *B*, $\Delta[Ca^{2+}]_i$ (left) and T_{50} (right) were larger in IB_4+ ($n = 136$) than in IB_4- ($n = 95$) neurons. *C*, $\Delta[Ca^{2+}]_i$ (left) and T_{50} (right) were larger in CAP+ ($n = 127$) than in CAP– ($n = 118$) neurons. Data from *A*, *B* and *C* were from both unlabelled and DiI-labelled DRG neurons. Similar results were obtained in cutaneous DRG neurons (DiI-positive) innervating glabrous skin of the hindpaw (*D*, *E* and *F*). *D*, $\Delta[Ca^{2+}]_i$ and T_{50} were the largest in small-, and the smallest in large-diameter cutaneous neurons ($n = 19$, 16, and 18 in small-, medium-, and large- diameter cell groups). *E*, $\Delta[Ca^{2+}]_i$ and T_{50} were larger in IB_4+ ($n = 27$) than in IB_4- ($n = 26$) cutaneous neurons. *F*, $\Delta[Ca^{2+}]_i$ and T_{50} were larger in CAP+ ($n = 26$) than in CAP– ($n = 27$) cutaneous neurons. Differences between groups were all statistically significant ($^*P < 0.05$, $^{**}P < 0.01$). Similar results were also obtained when Ca^{2+} transients were evoked with 4 s voltage steps from −60 to 0 mV in neurons under voltage clamp. $\Delta[Ca^{2+}]_i$ and T_{50} were the largest in small-, and the smallest in large-diameter neurons (*G*, $n = 10$ in small-, 9 in medium- and 7 in large-diameter groups); They were larger in IB_4+ ($n = 13$) than in IB_4- ($n = 13$) DRG neurons (*H*) and they were larger in CAP+ ($n = 17$) than in CAP– ($n = 9$) DRG neurons (*I*). Statistically significant differences between groups are indicated ($^*P < 0.05$, $^{**}P < 0.01$).

Table 1. Ca^{2+} transients in subpopulations of small-diameter DRG neurons

Subpopulation	*n*	$\Delta[Ca^{2+}]_i$ (nM)	T_{50} (s)
IB4+	96	445 ± 52	12.4 ± 0.9**
IB4−	31	416 ± 21	6.2 ± 0.5
CAP+	85	395 ± 19*	10.8 ± 0.9
CAP−	42	482 ± 45	11.1 ± 1.3
IB4+/CAP+	65	397 ± 20	12.0 ± 1.2
IB4+/CAP−	31	458 ± 50	13.2 ± 1.6
IB4−/CAP+	20	390 ± 57	6.7 ± 0.7
IB4−/CAP−	11	548 ± 97	5.2 ± 0.7

The magnitude ($\Delta[Ca^{2+}]_i$) and decay (T_{50}) of high-K^+-evoked Ca^{2+} transients were analysed in subpopulations of small-diameter (i.e. < 30 μm) DRG neurons. Subpopulations were defined by IB_4 binding, capsaicin (CAP) sensitivity, or the combination of the two and differences between groups (i.e. IB_4+ *versus* IB_4–) were assessed. The decay of evoked Ca^{2+} transients was significantly (**$P < 0.01$) slower in IB_4+ neurons than in IB_4– neurons. The magnitude of the evoked Ca^{2+} transient was significantly (*$P < 0.05$) smaller in CAP+ neurons than that in CAP– neurons. There was a significant ($P < 0.01$) group effect in the decay of evoked Ca^{2+} transients when subpopulations defined by the combination of IB_4 binding and CAP sensitivity were compared. *Post hoc* analysis indicated that the decay of the transient in IB_4+/CAP– neurons was significantly slower than that in IB_4–/CAP+ ($P < 0.05$) and IB_4–/CAP– neurons ($P < 0.05$). There were no other significant differences between groups.

Table 2. Ca^{2+} transients in subpopulations of medium-diameter DRG neurons

Subpopulation	*n*	$\Delta[Ca^{2+}]_i$ (nM)	T_{50} (s)
IB4+	96	331 ± 29**	8.9 ± 1.2**
IB4−	31	113 ± 11	3.5 ± 0.3
CAP+	85	319 ± 31**	8.2 ± 1.1
CAP−	42	166 ± 29	5.5 ± 1.5
IB4+/CAP+	65	344 ± 32	8.6 ± 1.3
IB4+/CAP−	31	271 ± 71	10.3 ± 4.1
IB4−/CAP+	20	115 ± 26	5.1 ± 1.1
IB4−/CAP−	11	113 ± 13	3.0 ± 0.2

The magnitude ($\Delta[Ca^{2+}]_i$) and decay (T_{50}) of high-K^+-evoked Ca^{2+} transients were analysed in subpopulations of medium-diameter (i.e. 30–40 μm) DRG neurons. Subpopulations were defined by IB_4 binding, capsaicin (CAP) sensitivity or the combination of the two, and differences between groups (i.e. IB_4+ *versus* IB_4–) were assessed. The magnitude was significantly larger (**$P < 0.01$) and the decay of evoked Ca^{2+} transients was significantly (**$P < 0.01$) slower in IB_4+ neurons than in IB_4– neurons. The magnitude of the evoked Ca^{2+} transient was significantly (**$P < 0.01$) larger in CAP+ neurons than that in CAP– neurons. There was a significant ($P < 0.01$) group effect in the magnitude of evoked Ca^{2+} transients when subpopulations defined by the combination of IB_4 binding and CAP sensitivity were compared. *Post hoc* analysis (Tukey test) indicated that the magnitude of the transient in IB_4+/CAP+ neurons was significantly larger than that in IB_4–/CAP + ($P < 0.05$) and IB_4–/CAP– neurons ($P < 0.01$). There were no other significant differences between groups.

evoked Ca^{2+} transients when classified according to cell body diameter, IB_4 binding, and CAP responsiveness, DiI+ neurons were not analysed separately in subsequent experiments.

In order to explore the possibility that IB_4 binding and CAP responsiveness could be used to identify unique subpopulations of small- and medium-diameter DRG neurons, these two criteria, as well as the combination of the two, were used to define subpopulations of DRG neurons initially defined by cell body diameter. Table 1 contains the results of this analysis, in which the magnitude and decay of high-K^+-evoked Ca^{2+} transients were compared between subpopulations of small-diameter DRG neurons. Table 2 contains the results of this analysis for medium-diameter neurons. In small-diameter DRG neurons, evoked Ca^{2+} transients decayed more slowly in IB_4+ neurons, while the magnitude of evoked transients was larger in CAP– DRG neurons. Results of this analysis raise the possibility that there are large Ca^{2+} transients in a subpopulation of non-nociceptive small-diameter DRG neurons. However, the largest and most slowly decaying Ca^{2+} transients in medium-diameter DRG neurons were present in putative nociceptors (i.e. IB_4+ and/or CAP+ neurons).

The consistency of the high-K^+-evoked changes in membrane potential observed in current clamp experiments could be used to argue against a role for excitability differences among DRG neurons as an explanation for differences among subpopulations of DRG neurons with respect to magnitude and decay of high-K^+-evoked Ca^{2+} transients. However, in order to further address this issue, a group of neurons was studied in voltage clamp. The perforated-patch technique was employed in order to establish whole-cell access, while minimizing the impact of the recording on the intracellular milieu (Horn & Marty, 1988). Resting $[Ca^{2+}]_i$ levels at a holding potential of −60 mV were similar to those observed in intact cells when subgrouped according to cell body diameter, IB_4 binding and CAP responsiveness (data not shown). A 4 s voltage step from −60 mV to 0 mV was associated with an increase in $[Ca^{2+}]_i$ in all of neurons tested. Examples of Ca^{2+} transients evoked with a 4 s voltage step to 0 mV in small-, medium- and larger-diameter neurons are shown in Fig. 2*F–H*, respectively. The voltage-step-evoked increase in $[Ca^{2+}]_i$ in subpopulations of DRG neurons was qualitatively and quantitatively similar to that observed in unclamped neurons in response to high K^+ (Fig. 3*G–I*). Differences between groups were statistically significant ($P < 0.05$ or $P < 0.01$, one-way ANOVA or Student's *t* test). However, there were no statistically significant differences between

subpopulations of DRG neurons with respect to the Ca^{2+} transients evoked with high K^+ in unclamped neurons and voltage steps in voltage-clamped neurons ($P > 0.05$, two-way analysis of variance).

Differences among subpopulations with respect to Ca^{2+} current density

Depolarization-induced increases in $[Ca^{2+}]_i$ in DRG neurons reflect an initial Ca^{2+} influx through voltage-gated Ca^{2+} channels (VGCC) (Shmigol *et al.* 1995*b*). In order to determine whether the differences among subpopulations of DRG neurons with respect to magnitude and decay of high-K^+-evoked Ca^{2+} transients reflect a differential density of voltage-gated Ca^{2+} current, voltage-gated Ca^{2+} currents were measured in subpopulations of cutaneous DRG neurons with whole-cell voltage clamp. Currents were evoked as described in Methods. High-voltage-activated Ca^{2+} current (HVACC) density was assessed by measuring peak Ca^{2+} current evoked at 0 mV (Fig. 4*A*) and dividing this value by cell capacitance. Typical *I–V* curves for Ca^{2+} currents evoked in small- (■), medium- (▲) and large- (●) diameter DRG neurons are shown in Fig. 4*B*. In contrast to high-K^+-evoked increases in $[Ca^{2+}]_i$, HVACC density was the smallest in small cells and the largest in large cells (Fig. 4*C*; $n = 55$, 41, and 19 for small-, medium-, and large-diameter neurons, respectively). The

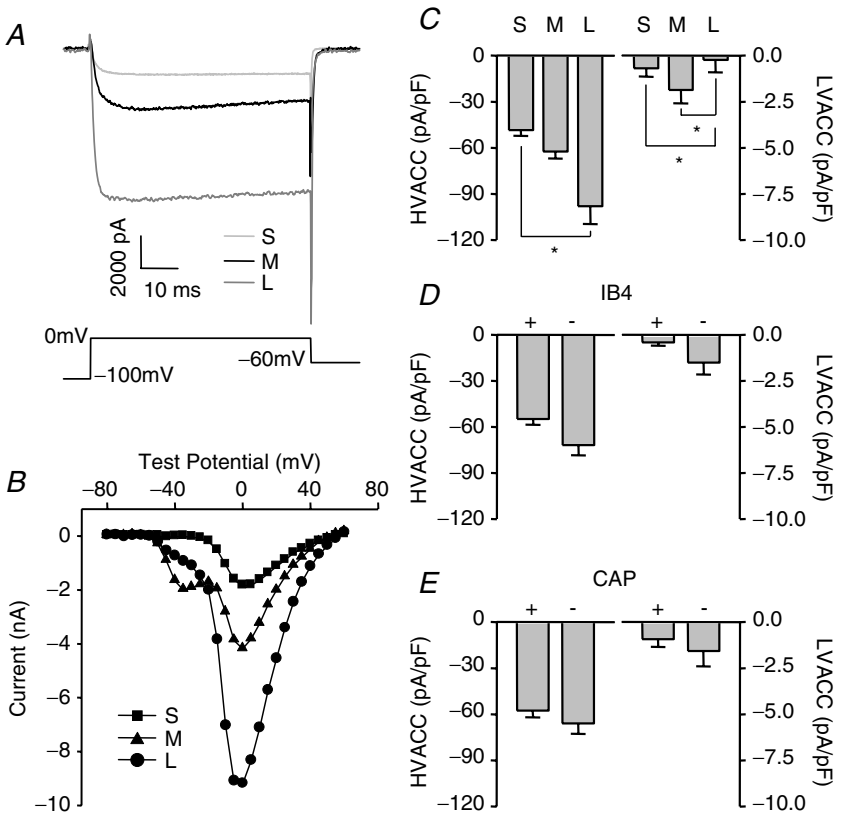

Figure 4. Differential distribution of voltage-gated Ca^{2+} currents among subpopulations of DRG neurons

A, Ca^{2+} current traces evoked at 0 mV from a holding potential of −60 mV in typical small- (light grey), medium- (black) and large- (dark grey) diameter DRG neurons, respectively. Current traces shown in *A* were part of families of traces used to generate the *I–V* curves shown in *B*, where data from the small- (S, ■), medium- (M, ▲) and large- (L, ●) diameter DRG neurons are plotted. The large low-voltage-activated Ca^{2+} current (LVACC), or T-type Ca^{2+} current, apparent in *I–V* data from the medium-diameter neuron was observed in 6 out of 41 (15%) medium-, 3 out of 19 (16%) large- and 2 out of 55 (4%) small-diameter neurons. *C*, high-voltage-activated Ca^{2+} current (HVACC) densities (left) were the smallest in small-, and the largest in large-diameter neurons ($n = 55$, 41, and 19 in small-, medium-, and large-diameter cell groups). LVACC densities (right) were smallest in large-, and largest in medium-diameter neurons. *D*, they were larger in IB_4- ($n = 60$) than in IB_4+ ($n = 48$) neurons. *E*, they were larger in CAP– ($n = 54$) than in CAP + ($n = 37$) neurons. The currents at 0 mV or at −50 mV were divided by cell capacitance to yield the HVACC or LVACC density. Statistically significant differences between groups are indicated (*$P < 0.05$).

difference in HVACC density between small and large cells was statistically significant ($P < 0.05$, one-way ANOVA). There were no statistically significant differences between subpopulations of DRG neurons defined by IB_4 binding (Fig. 4*D*; $n = 60$ for IB_4+ and 48 for IB_4- neurons) and CAP sensitivity (Fig. 4*E*; $n = 54$ for CAP+ and 37 for CAP– neurons) with respect to HVACC density ($P > 0.05$, Student's *t* test).

The presence of large (>100 pA) low-voltage-activated calcium current (LVACC) or T-type Ca^{2+} current was observed in 6 out of 41 (15%) medium-, 3 out of 19 (16%) large- and 2 out of 55 (4%) small-diameter neurons, respectively. Smaller (<100 pA at −50 mV) LVACC were detectable in both small- and medium-diameter DRG neurons. Differences between groups defined by cell body diameter were statistically significant ($P < 0.05$, one-way ANOVA, Fig. 4*C*) with respect to LVACC density. There were no significant differences between groups defined by IB_4 binding (Fig. 4*D*) or capsaicin sensitivity (Fig. 4*E*) with respect to LVACC density ($P > 0.05$, Student's *t* test).

CICR via RyR but not IP_3R contributes to evoked Ca^{2+} transients in medium- and large-diameter, IB_4- and CAP– neurons

Results from previous studies suggest that Ca^{2+}-induced Ca^{2+} release (CICR), from internal stores via ryanodine receptors (RyRs), contributes to the magnitude and duration of evoked Ca^{2+} transients in sensory neurons (Solovyova *et al.* 2002). Therefore, we sought to determine whether a differential distribution in the relative contribution of RyR-mediated CICR to high-K^+-evoked Ca^{2+} transients may contribute to observed differences among subpopulations of DRG neurons with respect to the magnitude and decay of high-K^+-evoked Ca^{2+} transients. After stable baseline responses to high K^+ were established, 10 μM ryanodine was added to the cell perfusate. Repeated 8 s applications of 10 mM caffeine were used to confirm block of RyRs. Neurons were then stimulated again with high K^+. Ryanodine alone had no influence on resting $[Ca^{2+}]_i$ level. The change in evoked increase in $[Ca^{2+}]_i$ in the presence of ryanodine was calculated as a percentage of baseline according to following equation:

$$\%\text{change in } \Delta[Ca^{2+}]_i = (\Delta[Ca^{2+}]_{i,\text{drug}} - \Delta[Ca^{2+}]_{i,\text{baseline}}) / \Delta[Ca^{2+}]_{i,\text{baseline}} \times 100.$$

The change in the decay of the evoked increase in $[Ca^{2+}]_i$ was calculated according to a similar equation:

$$\%\text{change in } T_{50} = (T_{50,\text{drug}} - T_{50,\text{baseline}}) / T_{50,\text{baseline}} \times 100.$$

Typical examples of evoked Ca^{2+} transients in small- (Fig. 5*A*) and large- (Fig. 5*B*) diameter DRG neurons were obtained before (continuous line) and during (dashed line) perfusion with normal bath solution containing 10 μM ryanodine. Two-way ANOVA of pooled data (Fig. 5*D–F*) revealed a significant drug effect on both magnitude ($P < 0.01$) and decay ($P < 0.05$) of evoked Ca^{2+} transients in all subpopulations of neurons analysed. There was also a significant interaction between subpopulation and drug effects on the magnitude of evoked Ca^{2+} transients when neurons were grouped according to cell body size ($P < 0.01$), IB_4 binding ($P = 0.01$) or CAP sensitivity ($P < 0.01$). That is, inhibition of RyRs resulted in a reduction in the magnitude of evoked increase in $[Ca^{2+}]_i$ in medium- ($n = 17$) and large- ($n = 10$) diameter, IB_4- ($n = 27$), and CAP– ($n = 26$) DRG neurons. There was also a significant interaction between subpopulation and drug effects on the decay of evoked Ca^{2+} transients in neurons grouped according to cell body size ($P < 0.05$). Of note, block of RyRs had no statistically significant effect in small-diameter ($n = 24$), IB_4+ ($n = 24$) and CAP+ ($n = 25$) subpopulations of DRG neurons. Application of ryanodine vehicle (bath solution containing 0.1% DMSO) had no significant influence on the magnitude or decay of evoked Ca^{2+} transients (Fig. 5*C–F*).

In addition to RyRs, there is evidence that IP_3 receptors may also be involved in Ca^{2+} release from internal stores (Svichar *et al.* 1997; Sanada *et al.* 2002; Solovyova & Verkhratsky, 2003). Therefore, the possibility that IP_3 receptors contribute to CICR in subpopulations of DRG neurons was assessed. Bath application of 100 μM 2-APB was used to block IP_3 receptors (Bootman *et al.* 2002). In order to confirm that this concentration of 2-APB was sufficient to block IP_3 receptor-mediated release of Ca^{2+}, UTP was used as a positive control because this compound has been shown to induce IP_3-mediated increases in $[Ca^{2+}]_i$ via P_2Y receptors in DRG neurons (Ralevic & Burnstock, 1998; Sanada *et al.* 2002). An example of results obtained from this experiment is shown in Fig. 6*A*. A brief (1.0 s) application of 100 μM UTP was used to evoke Ca^{2+} transients before (continuous line), during (short dashed line) and after (long dashed line) 2-APB (100 μM) perfusion. 2-APB clearly inhibited the increase in $[Ca^{2+}]_i$ induced by UTP. Examples of high-K^+-evoked Ca^{2+} transients in small and large neurons in the presence and absence of 100 μM 2-APB are shown in Fig. 6*B* and *C*. Pooled data were from 37 small-, 12 medium-, and 14 large-diameter neurons (Fig. 6*D*), from 32 IB_4+ and 31 IB_4- neurons (Fig. 6*E*), and from 30 CAP+ and 33 CAP– neurons (Fig. 6*F*). Blockade of IP_3 receptors by 2-APB had no statistically significant effects on the magnitude or decay of evoked Ca^{2+} transient in any of the subpopulations of DRG neurons studied.

SERCA plays a relatively large role in regulation of evoked Ca^{2+} transients in large-diameter, IB_4– and CAP– neurons

To further investigate the contribution of intracellular stores to the heterogeneity of evoked Ca^{2+} transients among DRG neurons, high-K^+-evoked Ca^{2+} transients were assessed before and after block of sarco/endoplasmic reticulum calcium ATPase (SERCA) with CPA (Thayer *et al.* 2002). Typical examples of evoked Ca^{2+} transients in small- (Fig. 7*A*) and large- (Fig. 7*B*) diameter DRG neurons were obtained before and during perfusion with

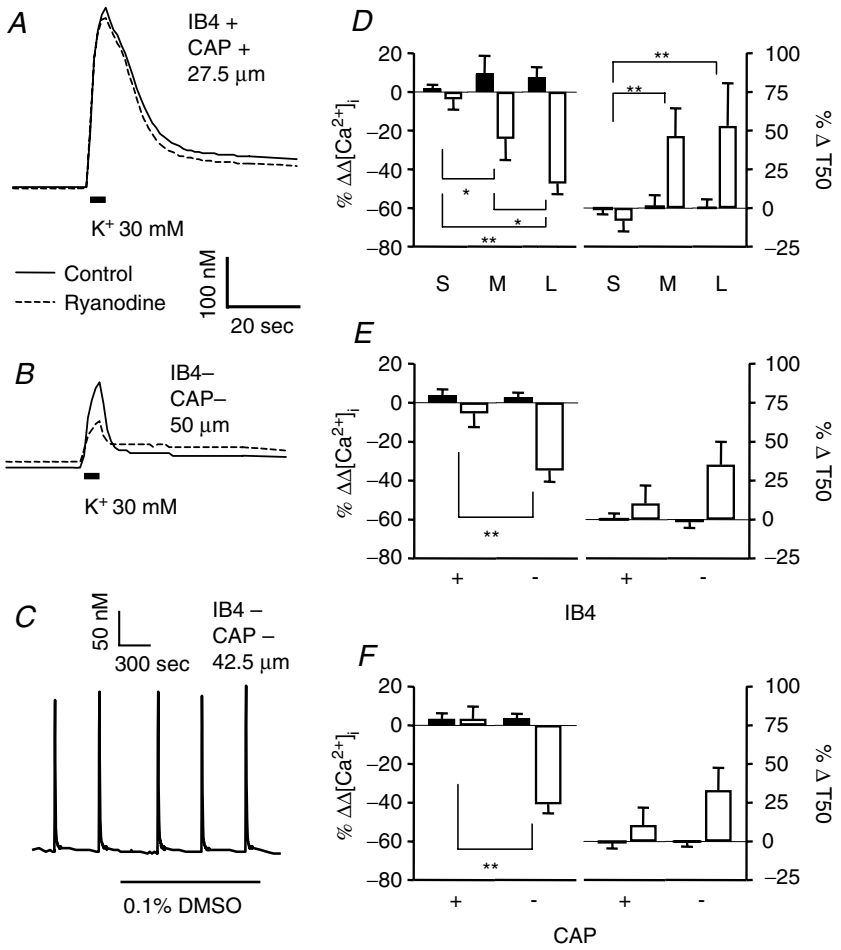

Figure 5. CICR via RyR contributes to evoked Ca^{2+} transients in large- and medium-cell body diameter, IB_4– and CAP– neurons

Typical evoked Ca^{2+} transients in small- (*A*) and large-diameter (*B*) DRG neurons were obtained before (continuous line) and during (dashed line) perfusion with normal bath solution containing 10 μM ryanodine. Note, prior to the second increase in $[Ca^{2+}]_i$ response, neurons were challenged with 10 mM caffeine repeatedly to establish block of RyRs. In order to determine the influence of ryanodine on the magnitude and decay of evoked Ca^{2+} transients, data were analysed as a percentage change from baseline which was determined for magnitude and decay as described in the text. Control neurons were treated with vehicle used to dissolve ryanodine (DMSO). *C*, An example of evoked Ca^{2+} transients from a large-diameter DRG neuron was obtained before and after perfusion with normal bath solution containing 0.1% DMSO. Pooled data for both control (filled bars) and drug-treated (open bars) neurons are plotted, illustrating the influence of ryanodine on the magnitude (left) and decay (right) of evoked Ca^{2+} transients in subpopulations of neurons defined by cell body size (*D*; $n = 24$ in small-, 17 in medium- and 10 in large-diameter cell groups), IB_4 binding (*E*; $n = 24$ in IB_4+ and 27 in IB_4– cell groups) and CAP sensitivity (*F*; $n = 25$ in CAP+ and 26 in CAP– cell groups). Data in each panel were analysed with a two-way ANOVA in order to assess the influence of subpopulation, drug treatment or an interaction between the two. Significant main effects associated with subpopulation and ryanodine were detected in each analysis. *Post hoc* analysis was performed if there was a significant interaction between main effects (subpopulation and ryanodine). Statistically significant differences between groups are indicated (*$P < 0.05$, **$P < 0.01$). Data for DMSO control were collected from 32 small-, 5 medium- and 6 large-diameter DRG neurons, which included 24 IB_4+, and 19 IB_4– neurons or 24 CAP+ and 19 CAP– neurons.

normal bath solution containing 5 μM CPA. CPA induced an increase in both the magnitude and decay of evoked Ca^{2+} transients. As expected, CPA also caused an increase in resting $[Ca^{2+}]_i$, which declined to some extent after the initial application of the compound, but did not return to the levels prior to CPA application. Two-way ANOVA of pooled data (Fig. 7*C*–*E*) revealed significant ($P < 0.01$) drug effects in all subpopulations of DRG neurons tested. There was also a significant interaction between subpopulation and drug effects on the magnitude of evoked Ca^{2+} transients when neurons were grouped according to cell body size ($P < 0.01$) and CAP sensitivity ($P < 0.01$). Inhibition of SERCA by CPA caused the largest increase in the magnitude of the evoked Ca^{2+} transient in large-diameter (Fig. 7*C*; $n = 44$ small-, 9 medium- and 16 large-diameter neurons) and CAP– (Fig. 7*E*; $n = 37$ CAP+ and 32 CAP– neurons) DRG neurons. A significant interaction was also detected on the decay of the evoked Ca^{2+} transient when neurons were grouped according to IB_4 binding ($P < 0.05$); the influence of CPA was larger in IB_4+ ($n = 40$) compared to IB_4– ($n = 29$) DRG neurons (Fig. 7*D*).

PMCA contributes minimally to the regulation of evoked Ca^{2+} transients in large-diameter, IB_4– and CAP– DRG neurons

Because Ca^{2+} efflux via plasma membrane Ca^{2+} ATPase (PMCA) may influence both the magnitude and decay of evoked increases in $[Ca^{2+}]_i$ (Thayer *et al.* 2002), the contribution of PMCA to the regulation of evoked Ca^{2+} transients among subpopulation of DRG neurons was determined. PMCA activity depends on direct

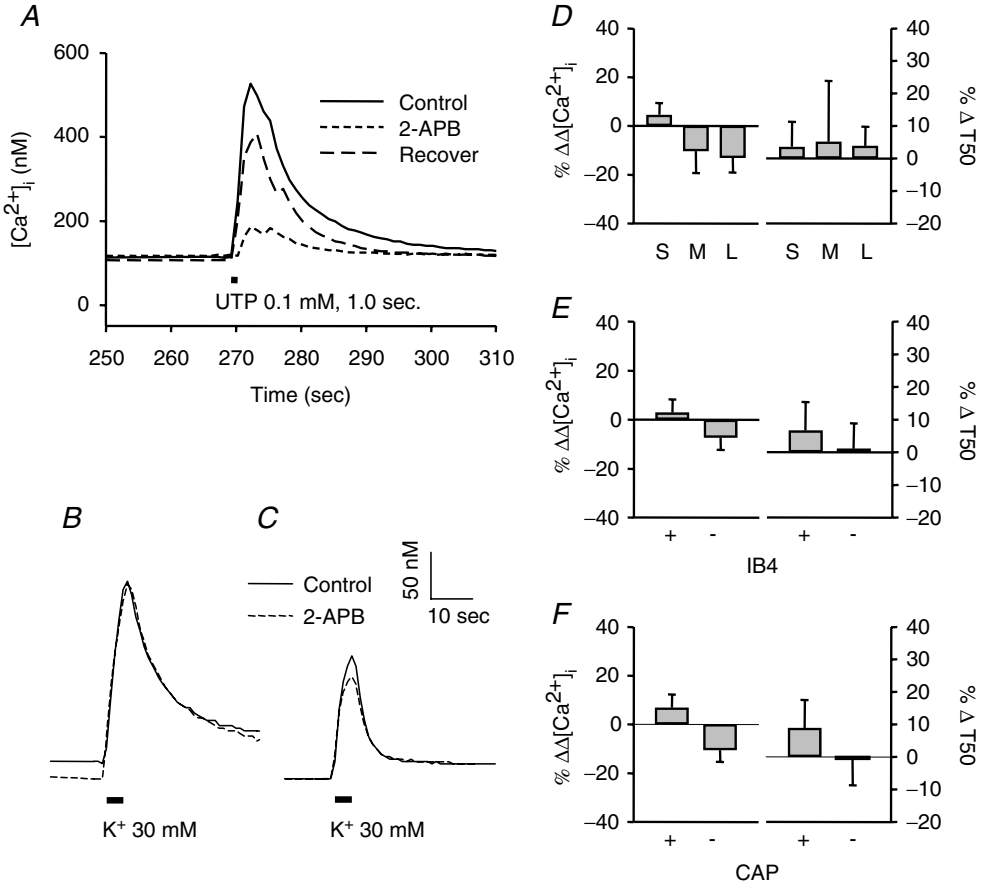

Figure 6. IP_3 receptors do not appear to contribute to evoked Ca^{2+} transients in DRG neurons
A, UTP-evoked increases in $[Ca^{2+}]_i$ were significantly attenuated by 2-APB in a reversible manner. Similar results were obtained in four neurons which responded to UTP application. However, high-K^+-evoked increase in $[Ca^{2+}]_i$ were not significantly influenced by 2-APB. Typical Ca^{2+} transients evoked in small- (*B*) and large- (*C*) diameter DRG neurons were obtained before (continuous line) and during (dashed line) perfusion with normal bath solution containing 100 μM 2-APB. The magnitude ($\Delta[Ca^{2+}]_i$) and decay (T_{50}) remained unchanged in all subpopulations of DRG neurons (*D*, *E* and *F*) during 2-APB treatment. Differences between groups were not statistically significant ($P > 0.05$). Data were collected from 37 small-, 12 medium- and 14 large-diameter DRG neurons, which included 32 IB_4+, and 31 IB_4– neurons or 30 CAP+ and 33 CAP– neurons.

interaction with calmodulin (Carafoli, 1992). It is therefore possible to block PMCA activity by blocking calmodulin binding. A peptide inhibitor, C28R2, has been developed for such a purpose (Enyedi *et al.* 1991; Enyedi & Penniston, 1993), and was used in the present study. C28R2 was commercially synthesized and chemically cross-linked to the viral transduction protein, TAT. Ca^{2+} transients were evoked in neurons that were preincubated (30 min) with 2 μM TAT-C28R2. Data for drug treatment were collected from 32 small-, 15 medium- and 8 large-diameter neurons, which included 35 IB_4+ and 20 IB_4– neurons or 30 CAP+ and 25 CAP– neurons. Control experiments were run in parallel and involved coverslips of DRG neurons that were handled identically, except for the omission of C28R2. Data for control were collected from 22 small-, 13 medium- and 11 large-diameter neurons, which included 20 IB_4+ and 26 IB_4– neurons or 20 CAP+ and 26 CAP– neurons. Two-way analysis of variance of pooled data (Fig. 8) revealed significant drug effect on both the magnitude ($P < 0.05$) and decay ($P < 0.05$) of evoked Ca^{2+} transients in each subpopulation of DRG neuron studied. There was a significant ($P < 0.05$) interaction between IB_4 binding and the influence of C28R2 on the magnitude of the high-K^+-evoked Ca^{2+} transients, which were larger in IB_4+ neurons in the presence of the drug than in IB_4– neurons. In order to determine whether the visual impression that C28R2 had little influence on large-diameter and IB_4– DRG neurons had statistical support, data were reanalysed as a percentage of control with one-way ANOVA (for size) or student's *t* tests (for IB_4 and CAP). Results of this analysis indicated that the influence of C28R2 was greater in medium-diameter ($P < 0.05$) and IB_4+ ($P < 0.01$) neurons than in larger-diameter neurons and IB_4– neurons, respectively.

NCX contributes minimally to the regulation of evoked Ca^{2+} transients in large-diameter, IB_4– and CAP– neurons

Ca^{2+} efflux via plasma membrane Na^+/Ca^{2+} exchangers (NCX) is another mechanism that may influence the magnitude and decay of evoked Ca^{2+} transients. Therefore, the role of NCX in the regulation of evoked Ca^{2+} transients among subpopulation of DRG neurons was assessed. NCX was inhibited by replacing extracellular Na^+ with Li^+ (Verdru *et al.* 1997). Examples of evoked Ca^{2+} transients in small- (Fig. 9*A*) and large- (Fig. 9*B*) diameter DRG neurons were obtained before and during perfusion with bath solution in which Na^+ had been replaced by Li^+. Li^+ did not change resting $[Ca^{2+}]_i$. Two-way ANOVA revealed a significant drug effect on both the magnitude ($P < 0.05$)

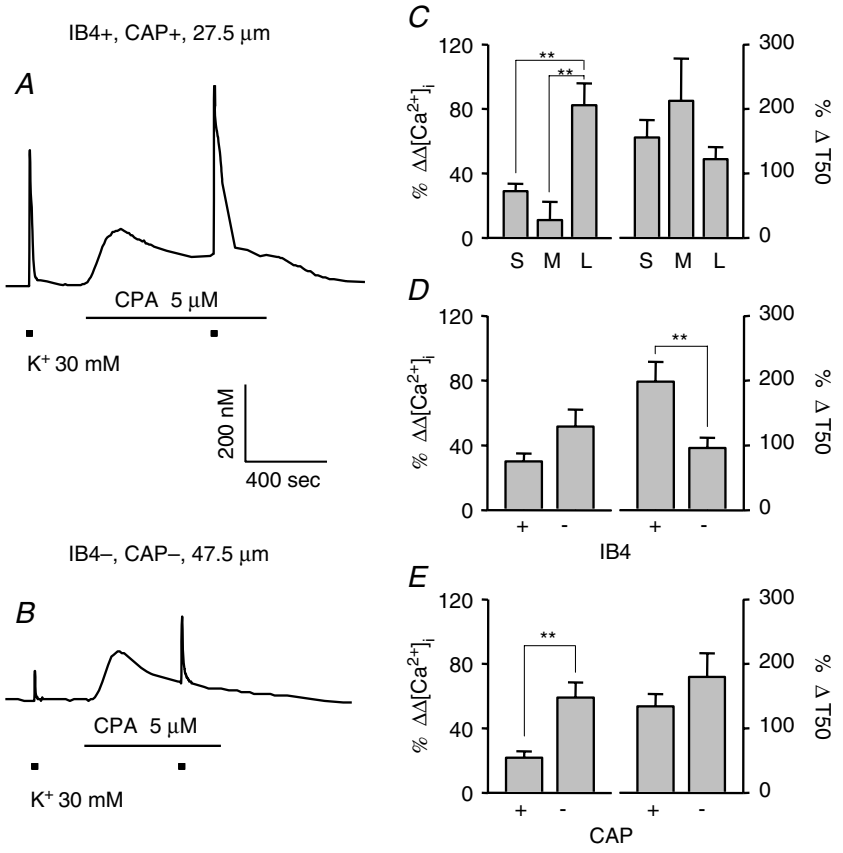

Figure 7. SERCA plays larger role in regulation of evoked Ca^{2+} transients in large-diameter, IB_4– and CAP– neurons
Typical evoked Ca^{2+} transients in small- (*A*) and large- (*B*) diameter DRG neurons were obtained before and during perfusion with normal bath solution containing 5 μM CPA, an inhibitor of sarco/endoplasmic reticulum Ca^{2+} ATPase. Pooled data for CPA-treated neurons are plotted, illustrating the influence of CPA on the magnitude (left) and decay (right) of evoked Ca^{2+} transients in subpopulations of neurons defined by cell body size (*C*, $n = 44$, 9, and 16 in small-, medium-, and large-diameter groups, respectively), IB_4 binding (*D*, $n = 40$ in IB_4+ and 29 in IB_4– groups) and CAP sensitivity (*E*, $n = 37$ in CAP+ and 32 in CAP– groups). Data from control neurons have been omitted for clarity. Data in each panel were analysed as in Figure 4 with a two-way ANOVA revealing significant main effects associated with subpopulation and CPA in each analysis. *Post hoc* analysis was performed if there was a significant interaction between main effects (subpopulation and CPA). Statistically significant differences between groups are indicated (** $P < 0.01$).

and decay ($P < 0.01$) of evoked Ca^{2+} transients in all three subpopulations of DRG neurons analysed. There were also significant interactions between subpopulation and drug effects on the magnitude of evoked Ca^{2+} transients when neurons were grouped according to IB_4 binding ($P < 0.01$) and CAP sensitivity ($P < 0.01$); Li^+ had a larger effect on the magnitude in IB_4+ ($n = 31$) and CAP+ ($n = 29$) neurons than in IB_4- ($n = 19$) and CAP– ($n = 21$) neurons, respectively (Fig. 9*D* and *E*). In addition, a significant interaction between subpopulation and drug effects on the decay ($P < 0.01$) of evoked Ca^{2+} transients was detected; *post hoc* analysis revealed that the Li^+-induced increase in decay was greater ($P < 0.05$) in medium- than in large-diameter neurons (Fig. 9*C*; $n = 28$ in small-, 13 in medium- and 9 in large-cell groups), in IB_4+ ($P < 0.01$) than in IB_4- neurons, and in CAP+ ($P < 0.01$) than in CAP– neurons (Fig. 9*D* and *E*).

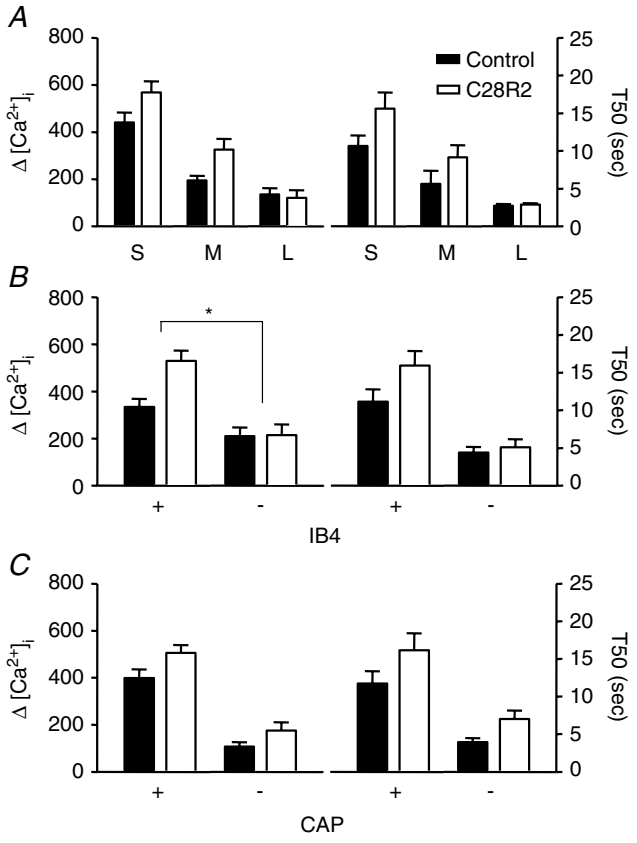

Figure 8. PMCA plays larger role in regulation of evoked Ca^{2+} transients in IB_4+ neurons
PMCA was blocked by 30 min preincubating neurons with the PMCA-specific peptide inhibitor C28R2 (2.0 μM). Control neurons were run in parallel. Pooled data for both control (filled bars) and drug treated (open bars) neurons are plotted, illustrating the influence of C28R2 on the magnitude (left) and decay (right) of evoked Ca^{2+} transients in subpopulations of neurons defined by cell body size (*A*), IB_4 binding (*B*) and CAP sensitivity (*C*). Data in each panel were analysed as in Fig. 4 with a two-way ANOVA revealing significant main effects associated with subpopulation and C28R2 in each analysis. *Post hoc* analysis was performed if there was a significant interaction between main effects (subpopulation and C28R2). Statistically significant differences between groups are indicated (*$P < 0.05$). Data for C28R2 treatment were collected from 32 small-, 15 medium- and 8 large-diameter DRG neurons, which included 35 IB_4+, and 20 IB_4- neurons, or 30 CAP+ and 25 CAP– neurons. Data for control were collected from 22 small-, 13 medium- and 11 large-diameter DRG neurons, which included 20 IB_4+, and 26 IB_4- neurons or 20 CAP+ and 26 CAP– neurons.

Mitochondria regulate evoked Ca^{2+} transients in all subpopulations of DRG neurons

With both Ca^{2+} transporter (uniporter) and Na^+/Ca^{2+} exchangers (MNCX), mitochondria may contribute to both uptake or release Ca^{2+}, and therefore are involved in the buffering of $[Ca^{2+}]_i$. Bath application of 10 μM CCCP was used to disrupt mitochondrial proton gradient and block both uptake and release of Ca^{2+} from mitochondria (Kostyuk *et al.* 1999). Typical examples of evoked Ca^{2+} transients in small- (Fig. 10*A*) and large- (Fig. 10*B*) diameter DRG neurons were obtained before and during perfusion with normal bath solution containing 10 μM CCCP. Pooled data are shown in Fig. 10*C*–*E*. Two-way ANOVA revealed a significant drug effect on both the magnitude ($P < 0.01$) and decay ($P < 0.01$) of evoked Ca^{2+} transients in all subpopulations of DRG neurons assessed. Furthermore, there was a significant interaction between the effects of subpopulation and drug with respect to the influence of CCCP on the magnitude of evoked Ca^{2+} transient when neurons were analysed according to cell body size ($P < 0.01$) and IB_4 binding ($P < 0.05$): the effects of CCCP were larger in medium- ($n = 6$, $P < 0.01$) and large- ($n = 9$, $P < 0.01$) diameter neurons than in small-diameter neurons ($n = 18$) (Fig. 10*C*) and in IB_4- ($n = 15$) neurons compared to IB_4+ ($n = 18$) neurons (Fig. 10*D*, $P < 0.01$). CCCP also caused an initial increase in resting $[Ca^{2+}]_i$, which declined to some extent with time, but did not returned to the levels prior to CCCP application.

Differences among subpopulations with respect to store-operated Ca^{2+} entry

In addition to initial Ca^{2+} influx through VGCCs and consequent Ca^{2+} release via RyRs from intracellular Ca^{2+} stores, store-operated Ca^{2+} entry (Usachev & Thayer, 1999) may also contribute to depolarisation-induced increase in $[Ca^{2+}]_i$ in DRG neurons. In order to determine whether the differences among subpopulations of DRG neurons with respect to evoked Ca^{2+} transients reflect a difference in store-operated Ca^{2+} entry, store-operated Ca^{2+} entry was measured in subpopulations of DRG neurons. Store-operated Ca^{2+} entry was induced by brief (20 s) application of normal bath solution (which contained 2.5 mM Ca^{2+}) in DRG neurons 10 min after depleting intracellular Ca^{2+} stores by treating neurons

with 10 μM CPA in Ca^{2+}-free bath solution. Representative recordings in Fig. 11*A* and *B* shows store-operated Ca^{2+} entry in small- and in large-diameter DRG neurons. Pooled data are plotted in Fig. 11*C–E*. The magnitude of the Ca^{2+} transient was significantly larger in small- ($n = 37$) than in medium- ($n = 15$, $P < 0.05$) or large- ($n = 12$, $p < 0.05$) diameter DRG neurons, and the decay of the Ca^{2+} transient was significantly slower in small-diameter than in medium-diameter neurons ($P < 0.05$; one-way ANOVA). The magnitude of the Ca^{2+} transient was larger ($P < 0.01$) and the decay slower ($P < 0.05$) in IB_4+ ($n = 39$) and CAP+ ($n = 36$) DRG neurons than in IB_4- ($n = 25$) or CAP– ($n = 28$) neurons, respectively (Student's *t* test).

Discussion

This study constitutes the first systematic analysis of evoked Ca^{2+} transients among subpopulations of DRG neurons. One of the most striking observations to arise from this analysis is that while there are no statistically significant differences among subpopulations of DRG neurons with respect to resting $[Ca^{2+}]_i$, there are marked differences among subpopulations with respect to both the magnitude and decay of evoked Ca^{2+} transients. The magnitude of the evoked increase in $[Ca^{2+}]_i$ was the largest, and the decay was the slowest in small-diameter, IB_4+ and CAP+ neurons while the magnitude was the smallest and the decay most rapid in large-diameter, IB_4- and CAP– DRG neurons. Similar results were also observed in cutaneous DRG neurons (DiI+) innervating the hindpaw when classified according to cell body diameter, IB_4 binding or CAP responsiveness. Importantly, similar results were also observed if Ca^{2+} transients were evoked with voltage steps. These observations suggested that there are differences among subpopulations of DRG neurons with respect to the mechanisms underlying the regulation of $[Ca^{2+}]_i$. Consequently, we assessed the contribution of a number of Ca^{2+} regulatory mechanisms to the magnitude and decay of evoked Ca^{2+} transients among subpopulations of DRG neurons. Results from this second series of experiments indicated that there are marked differences between subpopulations of DRG neurons with respect to a number of Ca^{2+} regulatory mechanisms including (1) voltage-gated Ca^{2+} currents; (2) RyR-mediated CICR; (3) SERCA; (4) PMCA; (5) NCX; and (6) store-operated Ca^{2+} entry.

The majority of the results in this study were obtained from intact (i.e. unclamped) neurons. It is important to point out that the study of unclamped neurons may have influenced our results in two important ways. First, in unclamped neurons, there may be

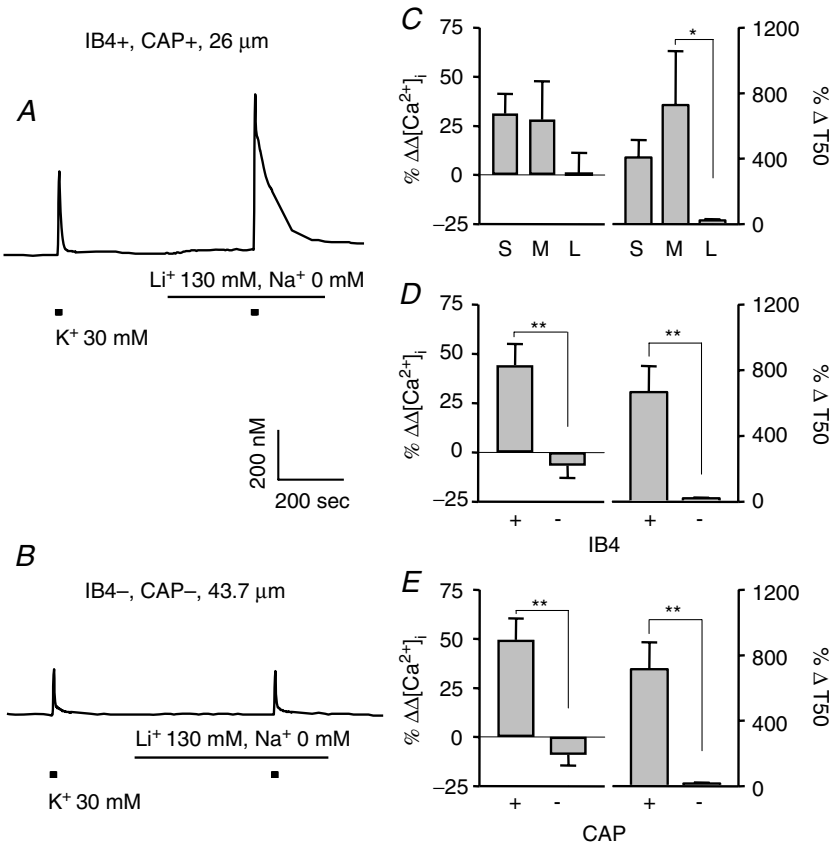

Figure 9. Na^+/Ca^{2+} exchange regulates evoked Ca^{2+} transients in IB_4+ and CAP+ neurons
Typical evoked Ca^{2+} transients in small- (*A*) and large-diameter (*B*) DRG neurons were obtained before and during perfusion with bath solution in which Na^+ had been replaced by Li^+. Pooled data illustrating the influence of Li^+ on the magnitude (left) and decay (right) of evoked Ca^{2+} transients in subpopulations of neurons defined by cell body size (*C*, $n = 28$, 13, and 9 in small-, medium-, and large-diameter groups, respectively), IB_4 binding (*D*, $n = 31$ in IB_4+ and 19 in IB_4- groups) and CAP sensitivity (*E*, $n = 29$ in CAP+ and 21 in CAP– groups). Data from control neurons were omitted for clarity. Data in each panel were analysed as in Fig. 4 with a two-way ANOVA revealing significant main effects associated with subpopulation and Li^+ in each analysis. *Post hoc* analysis was performed if there was a significant interaction between main effects (subpopulation and Li^+). Statistically significant differences between groups are indicated (*$P < 0.05$, ** $P < 0.01$).

differences between subpopulations of neurons with respect to resting membrane potential. Consistent with this suggestion, there was a trend in the current-clamp data set suggesting that the resting membrane potential was smallest in small-diameter neurons and largest in large-diameter neurons, and while the differences between groups in the present study were not statistically significant, we have reported that there are small, but significant differences between groups with respect to resting membrane potential (Gold *et al.* 1996). Resting membrane potential may influence high-K^+-evoked Ca^{2+} transients in two general ways: (1) by influencing the availability of voltage-gated Ca^{2+} channels, most dramatically low threshold, or T-type channels that are subject to steady-state inactivation; and (2) by influencing the availability of channels that have an impact on the excitatory response to membrane depolarisation, as both voltage-gated Na^+ current responsible for the upstroke of the action potential and voltage-gated K^+ currents that contribute to the downstroke of the action potential as well as the duration of the afterhyperpolarization are subject to steady-state inactivation. Second, variability in the action potential barrage and/or the time to membrane potential stabilization could have an impact on the magnitude of Ca^{2+} influx during this period of membrane potential instability, as well as the number of Ca^{2+} channels mediating influx during the plateau phase of the high-K^+-evoked membrane depolarization. Both of these factors may have contributed to variability in our data set as well as differences between subpopulations. Furthermore, it is possible that experimental manipulations designed to assess the impact of various influx, efflux and release pathways, influenced resting membrane potential and/or spike adaptation, and therefore, may have had an indirect influence on the magnitude and decay of the evoked Ca^{2+} transient. Conclusions drawn from these results are therefore made with caution.

While we acknowledge that the lack of clamp control may have influenced the magnitude and decay of the high-K^+-evoked Ca^{2+} transient in DRG neurons, we believe that the lack of clamp control is unlikely to have contributed significantly to the observed differences between subpopulations of DRG for the following reasons. First, our current-clamp data suggest that 'clamp control' was surprisingly good in the majority of neurons studied as high K^+ evoked more than two action potentials in only half of the small-diameter neurons studied, less than one-third of the medium-diameter neurons and none of the large-diameter neurons. Sustained activity was only observed in two medium-diameter neurons. Second, if one assumed that high-K^+-evoked action potentials resulted in larger and more slowly decaying Ca^{2+} transients, one

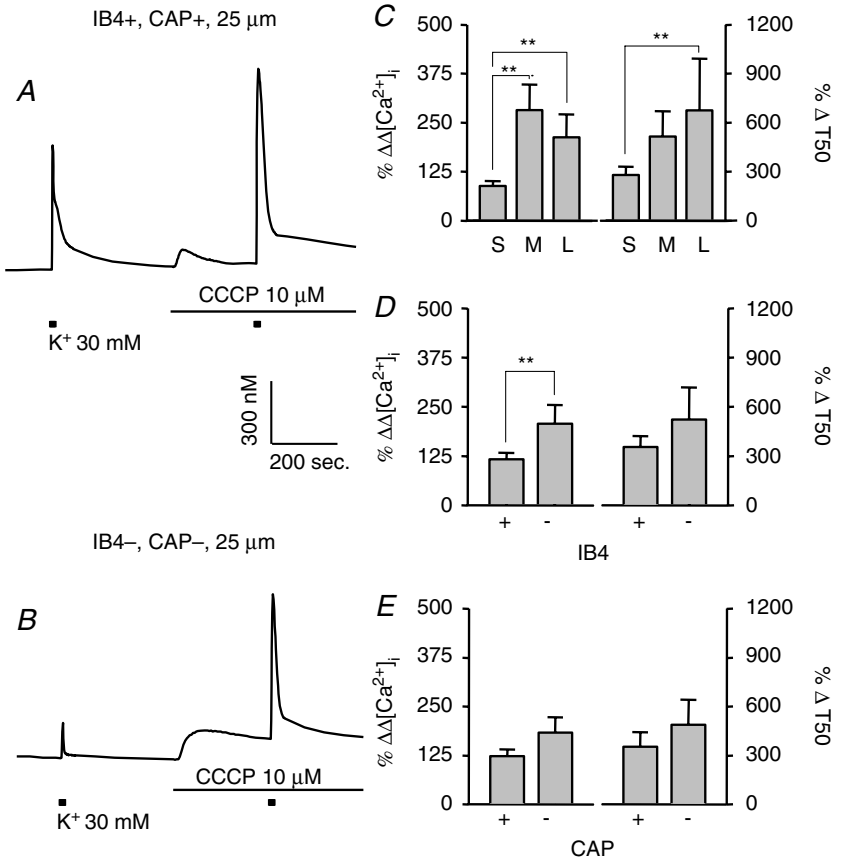

Figure 10. Mitochondria regulate evoked Ca^{2+} transients in all subpopulations of DRG neurons
Typical evoked Ca^{2+} transients in small- (*A*) and large- (*B*) diameter DRG neurons were obtained before and during perfusion with normal bath solution containing 10 μM CCCP, which disrupts mitochondrial proton gradient and blocks both uptake and release of Ca^{2+} from mitochondria. Pooled data illustrating the influence of CCCP on the magnitude (left) and decay (right) of evoked Ca^{2+} transients in subpopulations of neurons defined by cell body size (*C*, $n = 18$, 6, and 9 in small-, medium-, and large-diameter groups, respectively), IB_4 binding (*D*, $n = 18$ in IB_4+ and 15 in IB_4– groups) and CAP sensitivity (*E*, $n = 14$ in CAP+ and 19 in CAP– groups). Data from control neurons were omitted for clarity. Data in each panel were analysed as in Fig. 4 with a two-way ANOVA revealing significant main effects associated with subpopulation and CCCP in each analysis. *Post hoc* analysis was performed if there was a significant interaction between main effects (subpopulation and CCCP). Statistically significant differences between groups are indicated (** $P < 0.01$).

would predict that a subpopulation of small-diameter DRG neurons might have evoked Ca^{2+} transients that were similar to those observed in large-diameter DRG neurons. Yet the mean evoked increase in the lower quartile of small-diameter neurons (179 ± 11 nM), presumably reflecting small-diameter neurons that did not fire action potentials, was still statistically significantly larger than that in larger-diameter neurons. Third, Ca^{2+} transients evoked with voltage steps resulted in mean data that were qualitatively and quantitatively similar to those observed with high-K^+-evoked transients. And fourth, other investigators have also reported that evoked Ca^{2+} transients in unclamped DRG neurons are similar to evoked responses under voltage clamp (Werth *et al.* 1996; Usachev *et al.* 2002). It should also be noted the responses in unclamped neurons may be a better reflection of Ca^{2+} regulation *in vivo*, given the potential deleterious impact associated with the electrical access necessary for voltage clamp.

Our results indicate that there is a differential distribution of voltage-gated Ca^{2+} current density among subpopulations of DRG neurons. HVACC were present in the highest density in large-diameter, IB_4–, CAP– DRG neurons, and in the smallest density in small-diameter, IB_4+, CAP+ DRG neurons. Thus, the distribution of HVACC cannot account for the differences among subpopulations with respect to high-K^+-evoked Ca^{2+} transients. Rather, they suggest that if HVACC is the primary Ca^{2+} influx pathway responsible for initiating the Ca^{2+} transient in response to high K^+, then there must be mechanisms to amplify Ca^{2+} transients in some subpopulations of DRG neurons (i.e. small-diameter) and/or attenuate Ca^{2+} transients in other subpopulations of DRG neurons (i.e. large-diameter). Because LVACC were the highest in density in medium-, smaller in small- and smallest in large-diameter neurons, this differential distribution cannot account for the differences among subpopulations with respect to evoked Ca^{2+} transients either.

The relative contribution of CICR via RyRs to high-K^+-evoked Ca^{2+} transients observed in the present study differed among subpopulations of DRG neurons: the contribution was largest in large-diameter, IB_4–, and CAP– DRG neurons and virtually undetectable in small-diameter, IB_4+, or CAP+ DRG neurons. This observation was striking in light of what is believed to be the primary function of RyR-mediated CICR, which is to amplify increases in $[Ca^{2+}]_i$. Nevertheless, these results clearly indicate that the differential distribution of RyR-mediated CICR cannot account for differences among subpopulations of DRG neurons with respect to the magnitude and decay of evoked Ca^{2+} transients.

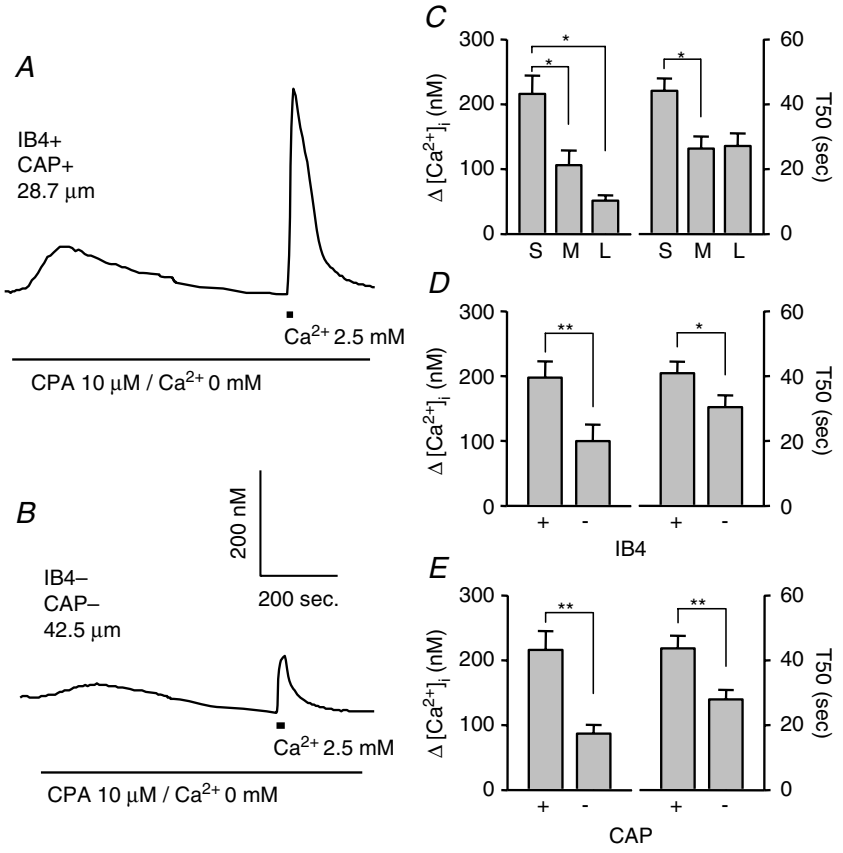

Figure 11. Store-operated Ca^{2+} entry among subpopulations of DRG neurons
Store-operated Ca^{2+} entry was induced with a brief (20 s) application of bath solution containing 2.5 mM Ca^{2+} after the treatment of neurons with Ca^{2+}-free solution containing 10 μM CPA. Shown in *A* and *B* are examples of such recordings made from small- (*A*) and large- (*B*) diameter DRG neurons. Pooled data illustrating the magnitude (left) and decay (right) of the Ca^{2+}-induced increase in $[Ca^{2+}]_i$ in subpopulations of neurons defined by cell body size (*C*), IB_4 binding (*D*) and CAP sensitivity (*E*) are plotted. Data in C ($n = 37$, 15, and 12 in small-, medium-, and large-diameter groups, respectively) were analysed with a one-way ANOVA, while data in *D* ($n = 39$ in IB_4+ and 25 in IB_4– groups) and *E* ($n = 36$ in CAP+ and 28 in CAP– groups) were analysed with a Student *t* test. Statistically significant differences between groups are indicated (*$P < 0.05$, **$P < 0.01$).

However, there are several mechanisms that may account for a differential influence of RyR-mediated CICR among subpopulations of DRG neurons. These include: proximity of RyRs to influx pathways given evidence for endoplasmic reticulum (ER) directly beneath the plasma membrane (Berridge, 1998); density/distribution of RyRs (Martone *et al.* 1997), which may be higher or more closely associated with influx pathways in large neurons; and isoforms of RyRs which appear to differ in Ca^{2+} conductance (Fessenden *et al.* 2000).

Our results with CPA suggests SERCA plays a larger role in large-diameter, IB_4–, and CAP– DRG neurons than in small-diameter, IB_4+, or CAP+ DRG neurons. SERCA-mediated sequestration in ER is thought to be initiated when the ER is depleted of Ca^{2+}. Thus, a larger role for SERCA in large-diameter, IB_4– and CAP– neurons is consistent with results obtained with ryanodine which indicated that Ca^{2+} release from the ER contributes to the evoked increase in $[Ca^{2+}]_i$. Importantly, these results may also begin to account for differences among subpopulations of DRG with respect to the magnitude and decay of evoked Ca^{2+} transients, which would be more readily attenuated by SERCA-mediated Ca^{2+} uptake in large-diameter, IB_4– and CAP– neurons. These results also raise the possibility that the extent to which ER stores are normally filled and/or filling capacity varies among subpopulations of DRG neurons, with a filling capacity that would be larger in large-diameter, IB_4–, and CAP– DRG neurons. Differences in the role of SERCA in evoked Ca^{2+} clearance among subpopulations of DRG neurons may also be explained, at least in part, by the relative density of SERCA and/or isoforms of SERCA (Thayer *et al.* 2002). Three different SERCA genes have been identified as well as four splice variants of SERCA2 (Vangheluwe *et al.* 2005). While there is evidence to suggest that SERCA2b is the only isoform present in neuronal tissue (Plessers *et al.* 1991; Van Den Bosch *et al.* 1999), this issue has not been systematically explored in DRG neurons.

NCX appeared to be involved in regulating the magnitude and, especially, the decay of evoked Ca^{2+} transients in small-diameter, IB_4+ and CAP+ neurons but not in large-diameter, IB_4– and CAP– DRG neurons. In contrast, PMCA had a larger influence on evoked Ca^{2+} transients in IB_4+ than in IB_4– DRG neurons. The primary function of both NCX and PMCA is to move Ca^{2+} from the inside to the outside of cells. The relative contribution of these Ca^{2+} efflux pathways suggests that neither contributes to differences among DRG neurons with respect to the magnitude and decay of evoked Ca^{2+} transients, both of which should enable evoked Ca^{2+} transients to recover faster in small-diameter, IB_4+, and CAP+ DRG neurons. This suggestion is made with caution, however, given that interventions used to block PMCA or NCX were non-specific, blocking all isoforms and splice variants of both efflux mechanisms. This lack of selectivity means that we may have missed an influence of isoforms and/or splice variants of these proteins in specific subpopulations of sensory neurons. For example, it is possible that a low-affinity isoform of the PMCA is present in high density in small-diameter, IB_4+ or CAP+ neurons, while a high-affinity isoform is present in large-diameter, IB_4– or CAP– neurons (Guerini, 1998; Usachev *et al.* 2002). This situation would enable PMCA to play a larger role in the the latter subpopulations than the former, under conditions associated with smaller increases in $[Ca^{2+}]_i$.

Our results with CCCP indicated that mitochondria contribute to regulation of both magnitude and decay of evoked Ca^{2+} transients in all subpopulations of DRG neurons assessed, although the influence on decay was greater in large-diameter, IB_4– and CAP– DRG neurons. Because mitochondria take up Ca^{2+}, particularly in the presence of high Ca^{2+} loads, and release Ca^{2+} as levels of $[Ca^{2+}]_i$ decrease, this organelle essentially filters Ca^{2+} transients, attenuating peak rises and prolonging the decay. The greater relative contribution of mitochondria in large-diameter, IB_4– and CAP– DRG neurons may contribute to observed differences among subpopulations of DRG neurons with respect to the magnitude and decay of evoked Ca^{2+} transients. However, this contribution is likely to be minimal, given that a larger contribution should have been associated with a smaller magnitude and a slower decay rate in large-diameter, IB_4– and CAP– DRG neurons; smaller values for both parameters were observed.

The last Ca^{2+} regulatory mechanism assessed in the present study was store-operated Ca^{2+} entry. This mechanism is thought to be activated following depletion of intracellular stores (Usachev & Thayer, 1999; Liu *et al.* 2003) as may occur following depolarisation-induced CICR (Solovyova *et al.* 2002), and is clearly present in sensory neurons (Usachev & Thayer, 1999; Liu *et al.* 2003). This mechanism appears to mediate both larger and more long-lasting increases in $[Ca^{2+}]_i$ in small-diameter, IB_4+ and CAP+ DRG neurons than in large-diameter, IB_4– or CAP– neurons. Consequently, this mechanism may be a primary mechanism underlying differences between subpopulations of DRG neurons with respect to the magnitude and decay of evoked Ca^{2+} transients. One problem with this suggestion, however, is that CICR appeared to contribute minimally to evoked Ca^{2+} transients in small-diameter, IB_4+ and CAP+ neurons, suggesting that there is little store depletion in these neurons with which to activate store-operated Ca^{2+} entry. However, the observation that SERCA appears to contribute to attenuation of the evoked Ca^{2+} transient in these subpopulations of DRG neurons, suggests that stores may not be filled to capacity under resting conditions in these neurons. If store-operated Ca^{2+} entry is activated following depletion of intracellular stores to some threshold level, it is possible that a small release of Ca^{2+}

from internal stores via CICR may be sufficient to activate store-operated Ca^{2+} entry. Additional experiments would be needed to further test this possibility.

The differential distribution of voltage-gated Ca^{2+} currents among subpopulations of cutaneous DRG neurons observed in the present study is consistent with results from previous studies (Scroggs & Fox, 1992*b*, 1992*a*), indicating HVACC were largest in large- and smallest in small-diameter DRG neurons. Similarly, the greatest density of LVACC were in medium-diameter DRG neurons (Scroggs & Fox, 1992*a*), with a relatively low density in small-diameter, putative nociceptive afferents (Cardenas *et al.* 1995; Blair & Bean, 2002).

Previous data suggest that on the one hand, CICR may contribute to evoked increase in $[Ca^{2+}]_i$ in a subpopulation of DRG neurons (Shmigol *et al.* 1995*b*), while on the other hand, RyR-mediated release from stores can be demonstrated in most DRG neurons (Usachev & Thayer, 1997). However the latter observation was made in the presence of a low concentration of caffeine which was used to sensitize RyRs. The observation that the all-or-none release of Ca^{2+} from ER depends on the presence of caffeine is suggested by results from another study in which Ca^{2+} influx and the concentration of free Ca^{2+} in the ER lumen were recorded simultaneously in the absence of caffeine (Solovyova *et al.* 2002). Under these conditions the amplitude of Ca^{2+} release from ER lumen was linearly dependent on Ca^{2+} current through VGCCs. We were also able to observe the involvement of RyR-mediated CICR in small-diameter, IB_4+ and CAP+ DRG neurons when caffeine was used to sensitive RyRs prior to the application of ryanodine (data not shown), supporting the suggestion that sensitization of RyRs is critical for observation of both the all-or-none response and the presence of RyR-mediated CICR in all DRG neurons. Importantly, these observations also support the suggestion that RyRs and/or RyR isoforms are differentially distributed among subpopulations of DRG neurons.

Results obtained with CPA in the present study are consistent with those reported in previous studies in sensory neurons. Both CPA (Usachev & Thayer, 1999) and thapsigargin (Shmigol *et al.* 1995*a*) have been used previously to block SERCA in DRG neurons, where application of either compound resulted in an increase in the magnitude and slowing of the decay of electrical and/or high-K^+-evoked Ca^{2+} transients. In neither study was a differential influence among subpopulations of DRG neurons reported, supporting the suggestion that this uptake mechanism is engaged by all DRG neurons.

The role of PMCA in regulating $[Ca^{2+}]_i$ in DRG neurons has been most extensively studied under conditions where the contribution of SERCA-mediated uptake was eliminated with blockers such as CPA. For example, inhibition of PMCA with elevated pH (Usachev *et al.* 2002) or the peptide inhibitor C28R2 (Werth *et al.* 1996) in the presence of a SERCA inhibitor indicate that this efflux mechanism contributes to recovery of evoked increases in $[Ca^{2+}]_i$ in sensory neurons. Interestingly, the relative contribution of this efflux pathway appears to be dynamically regulated. Large increases in $[Ca^{2+}]_i$ may result in a sustained ($\sim$1 h) increase in PMCA activity (Pottorf & Thayer, 2002). Activation of protein kinases may influence PMCA activity (Penniston & Enyedi, 1998; Usachev *et al.* 2002). The Ca^{2+} affinity of the pump also is influenced by alternative splicing of RNA encoding the C domain (Strehler, 1991). Four genes encoding PMCA have been identified, several of which result in splice variants. PMCA4 has PKA and PKC phosphorylation consensus sequences (Penniston & Enyedi, 1998) and alternative splicing of the same isoform influences Ca^{2+} affinity (Enyedi *et al.* 1994). PMCA4b and PMCA2a appear to be the dominant isoforms in sensory neurons (Usachev *et al.* 2002). Thus, it is possible that the relative contribution of PMCA to Ca^{2+} clearance among subpopulations of DRG neurons may depend on the extent of previous activity as well as on the splice variant, isoform present, and/or resting kinase and phosphatase activity.

Previous results suggest that there are differences among subpopulations of DRG neurons with respect to the relative contribution of NCX. Verdru *et al.* (1997) reported that inhibition of NCX by replacing external Na^+ with either Li^+ or TEA^+ dramatically slowed the decay of evoked Ca^{2+} transients in 'biphasic' but not in some 'monophasic' DRG neurons. Furthermore, blocking NCX resulted in an increase in resting $[Ca^{2+}]_i$ that was greater in biphasic than in monophasic rat DRG neurons (Verdru *et al.* 1997). These observations were in general similar to those obtained in the present study, given that biphasic cells were similar to IB_4+ or CAP+ neurons, and monophasic cells were similar to IB_4– or CAP– neurons. These previous observations also support the suggestion that the differential distribution of NCX among subpopulations of DRG neurons is unlikely to account for differences between subpopulations of DRG neurons with respect to properties of evoked Ca^{2+} transients.

Consistent with results of the present study, results from previous studies also indicate that there are differences among subpopulations of DRG neurons with respect to the relative contribution of mitochondrial Ca^{2+} buffering to evoked Ca^{2+} transients. For example, in experiments similar to those performed in the present study, application of CCCP to DRG neurons resulted in a larger increase in magnitude and slowing of the decay of high-K^+-evoked $[Ca^{2+}]_i$ transients in large- than in small-diameter DRG neurons (Shishkin *et al.* 2002). Similar results have also been reported in mouse DRG neurons (Kostyuk *et al.* 1999). Interestingly, when a higher concentration of K^+ (50 mM) was applied for longer periods of time (30 s) to DRG neurons cultured for 4–9 days, application of CCCP shortened the decay of the evoked Ca^{2+} transient

(Werth & Thayer, 1994). These results are consistent with the buffering of Ca^{2+} mediated by mitochondria, where under very high Ca^{2+} loads, the slow release of Ca^{2+} from mitochondria maintains elevated cytosolic Ca^{2+} levels. The shorter, less intense stimuli used in the present study appear to have been insufficient to engage the slow release mechanism in mitochondria to such an extent that it influenced the decay of the Ca^{2+} transient.

While we have identified at least three mechanisms that may contribute to differences among subpopulations of DRG neurons with respect to the regulation of evoked increase in $[Ca^{2+}]_i$, it is likely that other mechanisms may also contribute to these differences. One such mechanism is the presence of a high density of Ca^{2+}-binding proteins such as calbindin and parvalbumin. Indeed, there are a number of studies suggesting that these Ca^{2+}-binding proteins are differentially disturbed among sensory neurons, with parvalbumin preferentially expressed in neurons with a large cell body diameter, and calbindin expressed in neurons with a small cell body diameter (Honda, 1995; Ichikawa *et al.* 1997; Iino *et al.* 1998). Interestingly, parvalbumin is thought to have a much higher affinity for Ca^{2+} than calbindin (Chard *et al.* 1993). Thus, a relatively high density of parvalbumin in large-diameter DRG neurons would serve to attenuate high-K^+-evoked increases in $[Ca^{2+}]_i$, while the relative dearth of this protein in putative nociceptive afferents may enable relatively large evoked increases in $[Ca^{2+}]_i$.

The observation that putative nociceptors, CAP+ and/or IB_4+ DRG neurons with a small cell body diameter are more responsive to high K^+ than putative non-nociceptive DRG neurons seems somewhat paradoxical. High-threshold afferents should be less responsive than low-threshold afferents. However, we would suggest that the differential regulation of $[Ca^{2+}]_i$ makes sense in the context of the roles of these afferents *in vivo*. That is, nociceptive afferents are normally inactive, and are normally only activated by intense, potentially tissue-damaging stimuli. This activity initiates a sequence of events that impact the entire neuron as well as the organism. Activation of nociceptive afferents leads to transmitter release at both central and peripheral terminals, driving nociceptive responses centrally and neurogenic inflammatory responses peripherally. This activation may be associated with changes in excitability, which reflect a shift in the balance of kinase and phosphatase activity, resulting in changes in ion channel properties. This activation may also lead to changes in gene expression. A large increase in $[Ca^{2+}]_i$ may contribute to each of these processes (Berridge, 1998). On the other hand, low-threshold afferents are highly active, and able to sustain large bursts of activity. Stability in response properties and transmitter release are critical for high-fidelity encoding of low-threshold stimuli. Thus, small increases in $[Ca^{2+}]_i$ driving changes in kinase/phosphase activity, stimulus response properties, transmitter release and gene expression would all work against a highly stable low-threshold afferent output.

In summary, we have observed marked differences among subpopulations of neurons defined by cell body size, IB_4 binding and capsaicin sensitivity with respect to the magnitude and decay of evoked Ca^{2+} transients. The differences were not due to differences in the density of voltage-gated Ca^{2+} channels or the relative contribution of RyR-mediated CICR. Differences in the relative contribution of SERCA, mitochondia and store-operated Ca^{2+} entry may have contributed. Furthermore, differences in PMCA and NCX may have contributed, particularly if there were splice variants/isoforms expressed among subpopulations of neurons, although future experiments are needed to explore this possibility. Finally, these results suggest that electrical activity in subpopulations of DRG neurons will have a differential influence on Ca^{2+}-regulated phenomena such as spike adaptation, transmitter release and gene transcription. Significantly more activity should be required in large-diameter non-nociceptive afferents than that in small-diameter nociceptive afferents to have a comparable influence on these processes.

References

Berridge MJ (1998). Neuronal calcium signaling. *Neuron* **21**, 13–26.

Berridge MJ, Lipp P & Bootman MD (2000). The versatility and universality of calcium signalling. *Nat Rev Mol Cell Biol* **1**, 11–21.

Blair NT & Bean BP (2002). Roles of tetrodotoxin (TTX) -sensitive Na^+ current, TTX-resistant Na^+ current, and Ca^{2+} current in the action potentials of nociceptive sensory neurons. *J Neurosci* **22**, 10277–10290.

Bootman MD, Collins TJ, Mackenzie L, Roderick HL, Berridge MJ & Peppiatt CM (2002). 2-aminoethoxydiphenyl borate (2-APB) is a reliable blocker of store-operated Ca^{2+} entry but an inconsistent inhibitor of InsP3-induced Ca^{2+} release. *FASEB J* **16**, 1145–1150.

Caffrey JM, Eng DL, Black JA, Waxman SG & Kocsis JD (1992). Three types of sodium channels in adult rat dorsal root ganglion neurons. *Brain Res* **592**, 283–297.

Carafoli E (1992). The plasma membrane calcium pump. Structure, function, regulation. *Biochim Biophys Acta* **1101**, 266–267.

Cardenas CG, Del Mar LP & Scroggs RS (1995). Variation in serotonergic inhibition of calcium channel currents in four types of rat sensory neurons differentiated by membrane properties. *J Neurophysiol* **74**, 1870–1879.

Chard PS, Bleakman D, Christakos S, Fullmer CS & Miller RJ (1993). Calcium-buffering properties of calbindin D28k and parvalbumin in rat sensory neurones. *J Physiol* **472**, 341–357.

Dirajlal S, Pauers LE & Stucky CL (2003). Differential response properties of IB(4)-positive and – negative unmyelinated sensory neurons to protons and capsaicin. *J Neurophysiol* **89**, 513–524.

Enyedi A, Filoteo AG, Gardos G & Penniston JT (1991). Calmodulin-binding domains from isozymes of the plasma membrane Ca^{2+} pump have different regulatory properties. *J Biol Chem* **266**, 8952–8956.

Enyedi A & Penniston JT (1993). Autoinhibitory domains of various Ca^{2+} transporters cross-react. *J Biol Chem* **268**, 17120–17125.

Enyedi A, Verma AK, Heim R, Adamo HP, Filoteo AG, Strehler EE & Penniston JT (1994). The Ca^{2+} affinity of the plasma membrane Ca^{2+} pump is controlled by alternative splicing. *J Biol Chem* **269**, 41–43.

Fessenden JD, Wang Y, Moore RA, Chen SR, Allen PD & Pessah IN (2000). Divergent functional properties of ryanodine receptor types 1 and 3 expressed in a myogenic cell line. *Biophys J* **79**, 2509–2525.

Gold MS, Dastmalchi S & Levine JD (1996). Co-expression of nociceptor properties in dorsal root ganglion neurons from the adult rat *in vitro*. *Neuroscience* **71**, 265–275.

Gold MS & Traub RJ (2004). Cutaneous and colonic rat DRG neurons differ with respect to both baseline and PGE2-induced changes in passive and active electrophysiological properties. *J Neurophysiol* **91**, 2524–2531.

Grynkiewicz G, Poenie M & Tsien RY (1985). A new generation of Ca^{2+} indicators with greatly improved fluorescence properties. *J Biol Chem* **260**, 3440–3450.

Guerini D (1998). The significance of the isoforms of plasma membrane calcium ATPase. *Cell Tissue Res* **292**, 191–197.

Harper AA & Lawson SN (1985). Conduction velocity is related to morphological cell type in rat dorsal root ganglion neurones. *J Physiol* **359**, 31–46.

Honda CN (1995). Differential distribution of calbindin-D28k and parvalbumin in somatic and visceral sensory neurons. *Neuroscience* **68**, 883–892.

Horn R & Marty A (1988). Muscarinic activation of ionic currents measured by a new whole-cell recording method. *J Gen Physiol* **92**, 145–159.

Ichikawa H, Jacobowitz DM & Sugimoto T (1997). S100 protein-immunoreactive primary sensory neurons in the trigeminal and dorsal root ganglia of the rat. *Brain Res* **748**, 253–257.

Iino S, Kato M, Hidaka H & Kobayashi S (1998). Neurocalcin-immunopositive neurons in the rat sensory ganglia. *Brain Res* **781**, 236–243.

Kao JP (1994). Practical aspects of measuring $[Ca^{2+}]$ with fluorescent indicators. *Meth Cell Biol* **40**, 155–181.

Kostyuk E, Svichar N, Shishkin V & Kostyuk P (1999). Role of mitochondrial dysfunction in calcium signalling alterations in dorsal root ganglion neurons of mice with experimentally-induced diabetes. *Neuroscience* **90**, 535–541.

Lawson SN (2002). Phenotype and function of somatic primary afferent nociceptive neurones with C-, Adelta- or Aalpha/beta-fibres. *Exp Physiol* **87**, 239–244.

Liu M, Liu MC, Magoulas C, Priestley JV & Willmott NJ (2003). Versatile regulation of cytosolic Ca^{2+} by vanilloid receptor I in rat dorsal root ganglion neurons. *J Biol Chem* **278**, 5462–5472.

Lu S-G & Gold MS (2005). Intracellular calcium regulation among subpopulations of rat DRG neurons. *J Pain* **6**, S11.

Martin HA, Basbaum AI, Kwiat GC, Goetzl EJ & Levine JD (1987). Leukotriene and prostaglandin sensitization of cutaneous high-threshold C- and A-delta mechanonociceptors in the hairy skin of rat hindlimbs. *Neuroscience* **22**, 651–659.

Martone ME, Alba SA, Edelman VM, Airey JA & Ellisman MH (1997). Distribution of inositol-1,4,5-trisphosphate and ryanodine receptors in rat neostriatum. *Brain Res* **756**, 9–21.

Nagy JI & Hunt SP (1982). Fluoride-resistant acid phosphatase-containing neurones in dorsal root ganglia are separate from those containing substance P or somatostatin. *Neuroscience* **7**, 89–97.

Penniston JT & Enyedi A (1998). Modulation of the plasma membrane Ca^{2+} pump. *J Membr Biol* **165**, 101–109.

Plessers L, Eggermont JA, Wuytack F & Casteels R (1991). A study of the organellar Ca^{2+}-transport ATPase isozymes in pig cerebellar Purkinje neurons. *J Neurosci* **11**, 650–656.

Pottorf WJ & Thayer SA (2002). Transient rise in intracellular calcium produces a long-lasting increase in plasma membrane calcium pump activity in rat sensory neurons. *J Neurochem* **83**, 1002–1008.

Priestley JV, Michael GJ, Averill S, Liu M & Willmott N (2002). Regulation of nociceptive neurons by nerve growth factor and glial cell line derived neurotrophic factor. *Can J Physiol Pharmacol* **80**, 495–505.

Ralevic V & Burnstock G (1998). Receptors for purines and pyrimidines. *Pharmacol Rev* **50**, 413–492.

Sanada M, Yasuda H, Omatsu-Kanbe M, Sango K, Isono T, Matsuura H & Kikkawa R (2002). Increase in intracellular Ca^{2+} and calcitonin gene-related peptide release through metabotropic P2Y receptors in rat dorsal root ganglion neurons. *Neuroscience* **111**, 413–422.

Scroggs RS & Fox AP (1992*a*). Calcium current variation between acutely isolated adult rat dorsal root ganglion neurons of different size. *J Physiol* **445**, 639–658.

Scroggs RS & Fox AP (1992*b*). Multiple Ca^{2+} currents elicited by action potential waveforms in acutely isolated adult rat dorsal root ganglion neurons. *J Neurosci* **12**, 1789–1801.

Shishkin V, Potapenko E, Kostyuk E, Girnyk O, Voitenko N & Kostyuk P (2002). Role of mitochondria in intracellular calcium signaling in primary and secondary sensory neurones of rats. *Cell Calcium* **32**, 121–130.

Shmigol A, Kostyuk P & Verkhratsky A (1995*a*). Dual action of thapsigargin on calcium mobilization in sensory neurons: inhibition of Ca^{2+} uptake by caffeine-sensitive pools and blockade of plasmalemmal Ca^{2+} channels. *Neuroscience* **65**, 1109–1118.

Shmigol A, Verkhratsky A & Isenberg G (1995*b*). Calcium-induced calcium release in rat sensory neurons. *J Physiol* **489** (3), 627–636.

Silverman JD & Kruger L (1990). Selective neuronal glycoconjugate expression in sensory and autonomic ganglia: relation of lectin reactivity to peptide and enzyme markers. *J Neurocytol* **19**, 789–801.

Solovyova N & Verkhratsky A (2003). Neuronal endoplasmic reticulum acts as a single functional Ca2+ store shared by ryanodine and inositol-1,4,5-trisphosphate receptors as revealed by intra-ER $[Ca^{2+}]$ recordings in single rat sensory neurones. *Pflugers Arch* **446**, 447–454.

Solovyova N, Veselovsky N, Toescu EC & Verkhratsky A (2002). Ca^{2+} dynamics in the lumen of the endoplasmic reticulum in sensory neurons: direct visualization of Ca^{2+}-induced Ca^{2+} release triggered by physiological Ca^{2+} entry. *EMBO J* **21**, 622–630.

Strehler EE (1991). Recent advances in the molecular characterization of plasma membrane Ca^{2+} pumps. *J Membr Biol* **120**, 1–15.

Svichar N, Shmigol A, Verkhratsky A & Kostyuk P (1997). InsP3-induced Ca^{2+} release in dorsal root ganglion neurones. *Neurosci Lett* **227**, 107–110.

Thayer SA, Usachev YM & Pottorf WJ (2002). Modulating Ca^{2+} clearance from neurons. *Front Biosci* **7**, d1255–d1279.

Thut PD, Wrigley D & Gold MS (2003). Cold transduction in rat trigeminal ganglia neurons in vitro. *Neuroscience* **119**, 1071–1083.

Usachev YM, DeMarco SJ, Campbell C, Strehler EE & Thayer SA (2002). Bradykinin and ATP accelerate Ca^{2+} efflux from rat sensory neurons via protein kinase C and the plasma membrane Ca^{2+} pump isoform 4. *Neuron* **33**, 113–122.

Usachev Y, Kostyuk P & Verkhratsky A (1995). 3-Isobutyl-1-methylxanthine (IBMX) affects potassium permeability in rat sensory neurones via pathways that are sensitive and insensitive to $[Ca^{2+}]_{in}$. *Pflugers Arch* **430**, 420–428.

Usachev YM & Thayer SA (1997). All-or-none Ca^{2+} release from intracellular stores triggered by Ca^{2+} influx through voltage-gated Ca^{2+} channels in rat sensory neurons. *J Neurosci* **17**, 7404–7414.

Usachev YM & Thayer SA (1999). Ca^{2+} influx in resting rat sensory neurones that regulates and is regulated by ryanodine-sensitive Ca^{2+} stores. *J Physiol* **519**, 115–130.

Van Den Bosch L, Verhoeven K, De Smedt H, Wuytack F, Missiaen L & Robberecht W (1999). Calcium handling proteins in isolated spinal motoneurons. *Life Sci* **65**, 1597–1606.

Vangheluwe P, Raeymaekers L, Dode L & Wuytack F (2005). Modulating sarco (endo) plasmic reticulum Ca^{2+} ATPase 2 (SERCA2) activity: Cell biological implications. *Cell Calcium* **38**, 291–302.

Verdru P, De Greef C, Mertens L, Carmeliet E & Callewaert G (1997). Na^{+}–Ca^{2+} exchange in rat dorsal root ganglion neurons. *J Neurophysiol* **77**, 484–490.

Vulchanova L, Riedl MS, Shuster SJ, Stone LS, Hargreaves KM, Buell G, Surprenant A, North RA & Elde R (1998). $P_{2\times3}$ is expressed by DRG neurons that terminate in inner lamina II. *Eur J Neurosci* **10**, 3470–3478.

Werth JL & Thayer SA (1994). Mitochondria buffer physiological calcium loads in cultured rat dorsal root ganglion neurons. *J Neurosci* **14**, 348–356.

Werth JL, Usachev YM & Thayer SA (1996). Modulation of calcium efflux from cultured rat dorsal root ganglion neurons. *J Neurosci* **16**, 1008–1015.

Acknowledgements

This work was supported by NIH grant NS 44992 (MSG). We thank Drs Daniel Weinreich and Tony Gover for many helpful discussions during the execution of these experiments and the preparation of this manuscript and for the generous gift of the TAT-C28R2.